Development of an Intravaginal pressure measurement device

Maria Luciana Monteiro Beirão

Dissertação de Mestrado

Supervisor: Dr. Rita Rynkevic

Co-supervisor: Prof. Dr. Mario Vaz

Co-supervisor: Prof. Dr. António A. Fernandes

Mestrado Integrado em Engenharia Mecânica

Setembro de 2021

Resumo

O prolapso de órgãos pélvicos é uma patologia que afecta uma larga porção da população feminina e que interfere com a práctica de atividades diárias e com o conforto das pacientes e em muitos casos requer tratamento e cirurgia. Actualmente o diagnóstico é geralmente efectuado por observação, o que cria subjectividades, tanto a nível dos resultados de uma análise individual, como na avaliação da evolução da patologia. Há, assim, uma dependência na experiência e memória do clínico. Existem alguns dispositivos médicos que pretendem efectuar uma avaliação quantitativa das propriedades biomecânicas, funcionais e a anatomia da cavidade pélvica de modo a proporcionar objectividade ao processo de diagnóstico, mas apresentam diversas limitações.

O objectivo do presente trabalho é desenvolver e validar um dispositivo capaz de fazer medições do perfil de pressão ao longo das paredes vaginais anterior e posterior de forma breve e confortável, permitindo uma detecção de prolapso dos órgãos pélvicos ainda em fases iniciais e um acompanhamento da evolução da doença, facilitando a escolha e avaliação de tratamento e, assim, prevenindo o agravamento. Será também utilizado para recolher dados sobre propriedades de tecidos para desenvolver algoritmos de machine learning e desenvolver modelos computacionais para avaliar técnicas de correcção de POP *in silico*.

O instrumento desenvolvido foi um espéculo bivalve em aço inoxidável adaptado à instalação de sensores nas faces exteriores das lâminas. Foi necessário ainda efectuar a calibração e o ajuste dos sensores bem como a selecção e compra de outros materiais para facilitar a utilização e fixação dos componentes do instrumento. Para efectuar a validação foram efectuados testes passivos em modelos vaginais de materiais sintéticos e testes *ex vivo* em tecidos vaginais animais. Os resultados obtidos foram comparados com as propriedades obtidas por ensaios de tracção das mesmas amostras.

Este instrumento demonstrou conseguir detectar diferenças nas propriedades dos materiais e nas dimensões das amostras, usando aberturas do espéculo fixas, onde a expansão das lâminas é mitigada pela elasticidade dos tecidos vaginais e as leituras são recolhidas à medida que essa mitigação decorre. Dados obtidos por medições com o instrumento foram proporcionais aos obtidos por ensaios de tracção ao longo das diferentes aberturas usadas, com os modelos sintéticos a apresentar resultados comparativamente mais baixos nos sensores, provavelmente devido à área de secção reduzida e ao relaxamento dos tecidos nos ensaios *ex vivo*. Este instrumento demonstrou resolver limitações encontradas em instrumentos anteriormente existentes e trabalhos futuros *in vivo* e em análises de clínica permitirão mais desenvolvimentos.

Development of an Intravaginal pressure measurement device

Abstract

Pelvic organ prolapse is a pathology that affects a large portion of the female population and interferes with everyday activities and patients' comfort, and in many cases, requires treatment and surgery. Currently, the diagnosis is generally made by observation, which creates subjectivity both in individual analyses and in the evaluation of the development of the condition. Therefore, there is a dependence on the experience and memory of the clinician. There are some medical devices available that aim to make a quantitative evaluation of the pelvic cavity's biomechanics, anatomy, and functional properties to lend objectivity to the diagnostic procedure; however, they have various limitations.

The objective of the present work is to develop and validate a device capable of taking pressure distribution measurements along the anterior and posterior vaginal wall in a brief and comfortable manner, to be used as an aid to current diagnostic methods, allowing for the detection of pelvic organ prolapse in earlier stages and the follow-up of the evolution of the disease, facilitating the choice and evaluation of treatments and therefore preventing the worsening of the condition.

The instrument developed is a stainless-steel bivalve speculum adapted to fit sensors on the outer faces of the blades. It was also necessary to make the calibration and adjustments to the sensors and choose and purchase additional materials to facilitate the use and attachment of components of the instrument. Passive tests were conducted on synthetic material and on *ex vivo* animal vaginal tissues to validate the device. The readings obtained in these trials were compared with the properties obtained from tensile tests of the same samples.

This device was shown to be able to detect differences in material properties and sample dimensions in passive tests by using fixed speculum dilations wherein the expansion of the instrument is mitigated by the elasticity of the vaginal tissues and readings are collected as this mitigation occurs. Data resulting from device measurements was proportional to tensile test results over the different dilations used, with synthetic models showing lower comparative sensor readings likely due to the reduced cross-section area and the relaxation of tissues in *ex vivo* tests. Limitations found in other devices were shown to be solved by this device and future *in vivo* and clinical trials will be necessary for further development.

Agradecimentos

Presto o meu reconhecimento à Doutora Rita Rynkevic minha orientadora durante o percurso de investigação. Agradeço a sua disponibilidade, simpatia e tempo que me dedicou. Agradeço aos meus coorientadores Professor Doutor António Augusto Fernandes e Professor Doutor Mário Augusto Pires Vaz, pela disponibilidade, gentileza e simpatia.

Ao Instituto de Ciência e Inovação em Engenharia Mecânica e Engenharia Industrial e à Faculdade de Engenharia da Universidade do Porto, que disponibilizaram todos os materiais necessários à realização deste trabalho. Ao Ministério da Ciência Tecnologia, e Ensino Superior, FCT, Portugal e Programa Operacional Competitividade e Internacionalização - POCI projeto "SPINMESH - Melt electrospinning of polymeric bioabsorbable meshes for pelvic organ prolapse repair" - POCI-01-0145-FEDER-029232 e projeto "PRECOGFIL- Filamentos dentados pre-tensionados para correção transvaginal do prolapso do compartimento anterior e posterior"- PTDC/EMD-EMD/2229/2020.

Ao Professor Doutor Renato Manuel Natal Jorge, ao Professor Doutor José Trigo Barbosa e ao Professor Doutor Marco Paulo Lages Parente por me terem aberto a porta da investigação.

Aos meus colegas de laboratório que tanto me ajudaram, especialmente à Andressa, que se mostrou sempre disponível com um sorriso contagiante.

Aos meus pais e à minha irmã pelo incondicional apoio, estímulo e amor ao longo do meu percurso académico. Sem eles, não teria sido possível.

Aos meus amigos que me motivaram e socorreram ao mínimo queixume.

A todos o meu mais profundo e sincero bem hajam!

Table of Contents

List of Figures

List of Tables

Abbreviations

IAP- Intraabdominal Pressure

IVP- Intravaginal Pressure

LAM- *Levator ani* Muscle

LH- *Levator hiatus*

PFD- Pelvic Floor Dysfunction

PFM- Pelvic Floor Muscle

PFPT- Pelvic Floor Physical Therapy

POP- Pelvic Organ Prolapse

POP-Q- Pelvic Organ Prolapse Quantification

SEM- Standard Error of the Mean

SUI- Stress Urinary Incontinence

VTI- Vaginal Tactile Imaging

1 Introduction

1.1 Context and Motivation

Pelvic Organ Prolapse (POP) is a common disorder that affects a large portion of the parous population, with most estimates around 40%. Most women affected by POP report no symptoms; however possible symptoms of this pathology cause great physical, social, and emotional discomfort and POP is the main risk factor for surgical interventions. These interventions are often associated with complications and repeat operations, some of which have led the American Food and Drug Administration to impose bans on the sales and distribution of surgical meshes intended for transvaginal repair. A significant economic impact is associated with these treatments, which could be mitigated with a more effective early diagnosis. Current diagnostic methods present limitations, from dependence on subjective symptoms to tactile measurements with little to no means of making objective quantifications (Kenton and Mueller 2006) (Daneshgari, Kong and Swartz 2008) (Subramanian, et al. 2009) (Jelovsek and Barber. 2006).

A correct diagnosis at an early stage is essential to avoid treatment failure, prevent the development of severe symptoms and thus a higher risk of complications. The need to understand the mechanical behaviour of pelvic floor soft tissue and the mechanism of prolapse development gave rise to the development of devices that could measure intravaginal pressure (IVP) and assess mechanical properties of the vaginal wall *in vivo.* However, current manual examination methods can't reliably evaluate and quantify the development of POP over time, and known measurement devices are not currently available on the market. The device prototypes explored in the previous section present many disadvantages that make widespread use difficult, such as high production cost due to the amount of sensors and other unique device requirements, possible discomfort to the patients on account of the fixed shape of the probes, unreliable measurements, lack of data acquisition software or machine learning models that would allow for an easy interpretation of the results by the physician to analyse the progression of the condition. Diagnostic methods which rely on a conscious strain by the patient result in varying effects of intraabdominal pressure (IAP) as different muscles may be activated, which may not allow for accurate measurement of the properties of the vaginal wall. Continuous straining during examinations may even worsen the condition in some cases (Bø 2012).

1.2 Objectives

The following work aims to assemble and validate a minimally invasive diagnostic tool for IVP measurements capable of acquiring load values of the anterior and posterior vaginal walls and overcoming the limitations found in previously analysed examples of devices.

1.3 Project methodology

This project was divided into the following stages:

- Bibliographic review and state of the art to understand and clarify the requirements of this device;
- Device assembling and adaptation according to requirements;
- Preparation of the operating device manual and measurement protocol;
- Device validation through experimental data.

1.4 Work structure

Chapter 2 describes an introduction to the pathology this device intends to diagnose as well as a few notions of the anatomy affected by said disease and its socio-economic impacts.

Chapter 3 presents known methods of diagnosis and assessment, first the conventional ones and their limitations, followed by alternative solutions currently in development.

Chapter 4 presents the motivation behind this work in light of the context explored in the previous bibliographic review

Chapter 5 describes the device used in this work and the experimental methods and protocols chosen to test it.

Chapter 5 presents the test results, followed by their analysis and discussion.

Finally, chapter 7 contains the conclusions and proposes future works to contribute to the further development of this device.

2 Overview of Pelvic Floor Anatomy and Dysfunction

2.1 Anatomy of the Female Pelvic Floor

Female pelvic floor is a complex group of bones, connective tissues, and muscles. The pelvic floor is divided into two compartments, anterior and posterior, separated by the vaginal walls attached to the pelvic sidewalls. The anterior compartment contains the bladder and urethra and is bound by the pelvic sidewalls, the pubic bones, and the anterior vaginal wall, whilst the posterior compartment contains the rectum and anus, and is bound by the perineal body, the posterior vaginal wall, and the sacrum (DeLancey 2016).

The *levator ani* muscles (LAM) (Figure 1) are a muscle group responsible for supporting the pelvic organs and keeping them closed by exerting forces that balance the differential between atmospheric and abdominal pressure and preventing the stretching and straining of connective tissues. Although opinions vary, the general consensus states that the LAM is divided into three regions according to their attachments: pubovisceral, puborectal and iliococcygeus. The mechanical function of each pelvic floor muscle (PFM) depends on its shape, attachment point and angle. These angled muscles are contracted at rest and produce forces with vertical and horizontal components meant to support the perineal structure and ensure closure of the *levator hiatus* (LH) respectively. The LH constitutes the passage for the urethra, vagina, and rectum and its injury, lengthening and widening contributes to the development of pelvic floor dysfunction (PFD) (DeLancey 2016) (Ashton-Miller, A. and DeLancey 2014) (Schwertner-Tiepelmann, et al. 2012) (Ghetti, et al. 2005) (Weber and Richter 2005) (Jelovsek, Maher and Barber 2007).

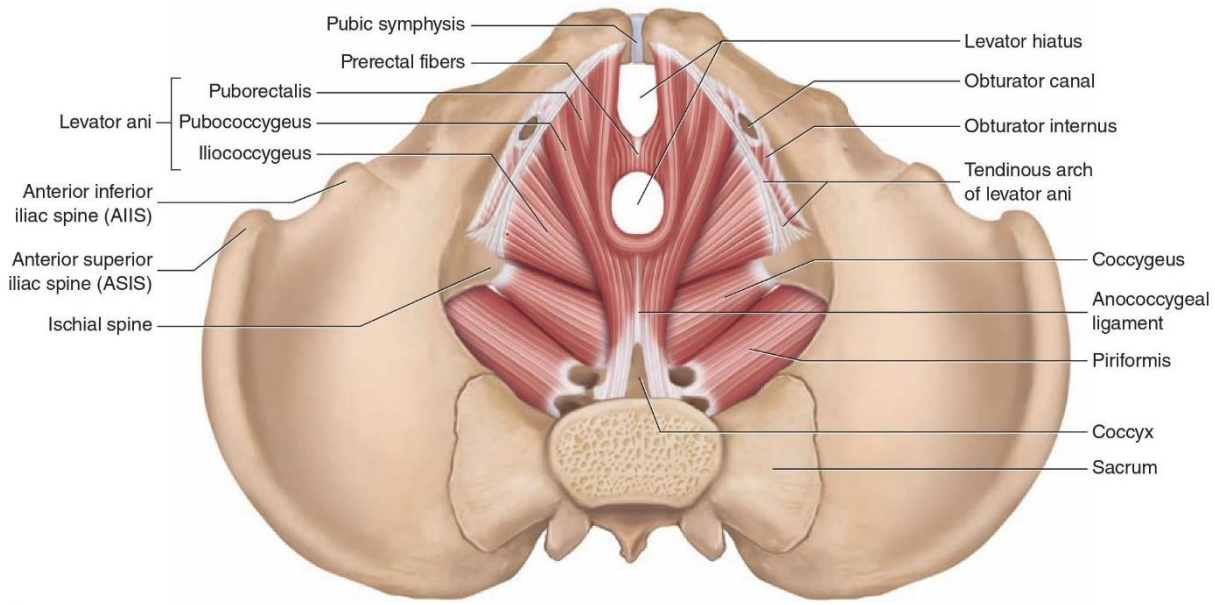

Figure 1: Female PFMs (Muscolino, J. E. 2014)

Other important pelvic components are the connective tissues which connect the vagina and the uterus to the pelvic walls and are divided into three levels. In level I, mesenteric structures suspend the upper third of the vagina and the cervix to the pelvic walls. In level II, the middle third of the vagina is attached laterally to fascial structures. Finally, in level III the distal third of the vagina is fused with the surrounding structures (DeLancey 2016).

The complex mechanical function of the female pelvic floor is to support the female pelvic organs and the unborn child and to control the opening of the bladder and rectum (continence) without interfering with micturition, defecation, sexual functions, and parturition. As it is

possible to see, each of the components above has a different function, understanding its role is fundamental to prevent and treat pelvic floor dysfunctions (Ashton-Miller, A. and DeLancey 2014).

2.2 Pelvic floor dysfunction

The dysfunction of the pelvic floor is understood as a complex of disorders. It affects the ligamentous apparatus and pelvic floor muscles that hold the pelvic organs in a normal position and provide urine and faeces containment. The percentage of women suffering from PFDs ranges from 30% to 50%, depending on the definition. PFDs mainly associated with parity and delivery mode, obesity, ageing, heredity, menopause, hormonal changes, severe physical exertion associated with increased intra-abdominal pressure, among others. The close anatomical relationship between the vaginal wall, bladder and rectum often contribute to the emergence of anatomical-functional failure of adjacent organs and systems. Pelvic organ prolapse (POP), various types of incontinence (urinary incontinence (UI), defecatory dysfunction), chronic cystourethritis, sexual dysfunctions remain the most common disorders in urogynaecology (Kenton and Mueller 2006) (Jundt, Peschers and Kentenich 2015) (Haylen 2010) (DeLancey 2016).

PFD Risk factors

Common risk factors include vaginal childbirth, genetic factors, oestrogen deficiency, smoking, prior surgery, loss of muscle mass with advanced age, increased body weight, chronically increased intraabdominal pressure, and an increased age of the mother upon delivery of the first child. Each consecutive vaginal delivery increases severity of POP and parity is the strongest risk factor. The use of forceps to aid delivery and a prolonged second stage of labour are also associated with a higher risk. Handa, *et al.* (2004) found that more so than BMI, a larger waist circumference is a stronger risk factor for certain types of POP possibly due to an increase in mechanical forces in the pelvic floor (Ghetti, et al. 2005) (Weber and Richter 2005) (Jelovsek, Maher and Barber 2007) (Schaffer, Wai and Boreham 2005).

Urinary incontinence

Urinary issues, such as stress urinary incontinence (SUI), is the involuntary loss of urine associated with increased intra-abdominal pressure during activities. Conventional treatments to cure SUI are: non-invasive - pelvic floor muscles (PFMs) training, minimally invasive - bulking methods, and invasive - surgical procedures using native tissues or implants. Surgical procedures are more likely to be implemented to cure urinary incontinence (UI). However, native tissue repair relates to anaesthesia risks and high recurrence rates (25%). In menopause, the lack of hormonal support depletes collagen reserve, being a possible explanation for the many surgical procedures' failure. The use of slings and meshes may cause postoperative complications (>15%), such as bleeding, erosions, urethral injury, infection, chronic pain. The SUI impairs women's quality-of-life and represents a significant public health problem, implying high costs due to its high prevalence (~ 35%). It is estimated that for the USA alone, the total number of women undergoing SUI surgery by 2050 will increase by 47.2%. These figures imply that the diagnosis and treatment of UI is an important matter, not just for the patient but also for the specialist (Haylen 2010) (Jundt, Peschers and Kentenich 2015) (Lazarou, Minis and Grigorescu 2019) (Rechberger, et al. 1998) (Blaivas, et al. 2015) (Wu, Kawasaki, et al. 2011).

Pelvic organ prolapse

Pelvic organ prolapse (POP) or urogenital prolapse is a common condition which consists of a type of hernia wherein the pelvic organs suffer a downward descent from their normal positions causing a protrusion. This is due to changes in the structure and function of the pelvic floor. Vaginal delivery causes direct trauma to the PF, and many women fail to recover completely. It is theorized that POP develops as the upper vagina is dislocated from an almost horizontal position to semi-vertical position, losing its normal function of balancing intraabdominal pressure, because of loss of tone in the LAM. This loss of tone can be caused by direct damage during the second stage of labour with the increased stretch of the muscles and possibly by neurological injury. POP may also be caused by damage to the vaginal wall by distention or by displacement of the vaginal wall upon loss of attachment to the pelvic side wall (DeLancey 2016) (Weber and Richter 2005) (Schaffer, Wai and Boreham 2005) (Bhadana 2020).

There is a correlation between POP and a decrease in smooth muscle of the vaginal wall though the mechanisms are unknown. Decreased collagen is associated with POP as it's the main component of connective tissue which supports the pelvic floor. A study conducted on excised mice vaginal tissue by Rahn, *et al.* (2008) theorized that an abnormal or decreased collagen content during pregnancy may alter the biomechanical properties of the vaginal wall, leading to an increased strain, decreased stiffness and a decreased maximal stress of the tissues. It was concluded by Michael H. Heit, et al. (2007) that the vaginal sidewall of women suffering from POP is more extensible than that of women with a healthy support whose tissues present a higher elastic modulus. POP symptoms may cause both physical discomfort and emotional distress due to its impact in patients' body image, both factors contributing to a decreased quality-of-life (Kerkhof, Hendriks and Brölmann 2009) (Schaffer, Wai and Boreham 2005) (Jelovsek and Barber. 2006).

Estimates of the percentage of the parous population affected by POP are usually between 30% and 50%. An easy way of accessing its incidence and severity is through the prevalence of POP surgery since it accounts for the number of severe cases. In the US, Jennifer M. Wu, *et al.* (2014) reported a lifetime cumulative risk of POP surgery of 12.6%. A 13 yearlong study by Mascarenhas, *et al.* (2015) using data from the Portuguese National Medical Registry found a prevalence of hospital admissions among women aged 55 to 74, with a mean age of 63.1 years. In 2012, 205 in 100,000 women over 65 years of age in Portugal went under surgery and in 2005, the number of POP surgical admissions per 100,000 women was 87 in Germany, 114 in France and 113 in England. The total cost of admissions for POP procedures in 2005 made up 0.1% of that year's national health system budget for England, 0.046% for France and 0.071% for Germany (Samuelsson, et al. 1999) (Hendrix, et al. 2002) (Subramanian, et al. 2009) (Department of Health 2009-10) (Clark 2007) (BASYS Beratungsgesellschaft für angewandte Systemforschung mbH, WifOR, Gesundheitsökonomisches Zentrum der TU Dresden (GÖZ), TU Berlin, IEGUS 2015).

POP Symptoms

Many patients with POP are asymptomatic and all possible symptoms are common to or may coexist with other forms of PFD which requires clinicians to be especially attentive when making a diagnosis. The presence of most known symptoms has a weak correlation with severity of prolapse, increasing the need for an objective evaluation. Richard C. Bump, et al. (1996) proposed a solution to the ambiguity of symptoms by dividing them into standard categories: urinary symptoms (stress incontinence, frequency, urgency, urge incontinence, hesitancy, weak or prolonged urinary stream, feeling of incomplete emptying, manual reduction of the prolapse to start or complete bladder emptying, and positional changes to start or complete voiding), bowel symptoms (difficulty with defecation, incontinence of flatus,

incontinence of liquid stool, incontinence of solid stool, fecal staining of underwear, urgency of defecation, discomfort with defecation, digital manipulation of vagina, perineum, or anus to complete defecation, feeling of incomplete evacuation, and rectal protrusion during or after defecation), sexual symptoms, and other local symptoms (vaginal pressure or heaviness, pain, sensation or awareness of tissue protrusion, sensation or awareness of tissue protrusion) (Jelovsek and Barber. 2006) (Bump, et al. 1996).

POP types

There are different forms of POP depending on which segment is affected, as illustrated in figure 2. The most common type of POP affects the anterior vaginal wall, causing the descent of the bladder (cystocoele). Cystocoele usually occurs some years after childbirth due to genital atrophy from aging, or less frequently in younger multiparous women. When the posterior vaginal wall is affected, there is a descent of the rectum and in some cases, the small or large bowel (rectocoele). This may occur during childbirth. Lastly, when the uterus or post-hysterectomy vaginal cuff are affected, apical prolapse occurs, leading to a protrusion of the small intestine (enterocoele), the bladder or the colon (sigmoidocoele) (Weber and Richter 2005) (Brunner, Smeltzer and Suddarth 2010).

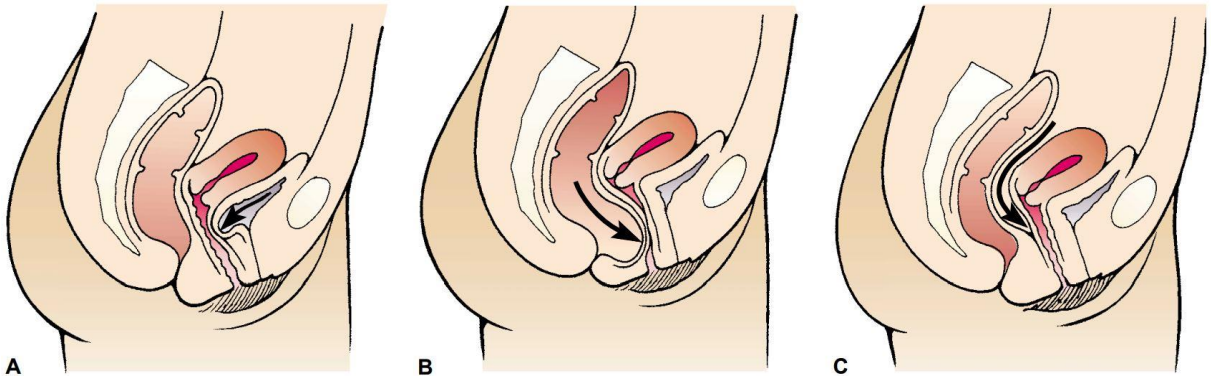

Figure 2: Most common types of POP: (A) cystocoele, (B) rectocoele, (C) enterocoele (Brunner, Smeltzer and Suddarth 2010)

POP also occurs in different levels of severity, depending on the distance travelled by six specific anatomical points (as shown in figure 3 two on the anterior vaginal wall, Aa and Ba, two on the superior vagina, C and D, and two on the posterior vaginal wall, Ap and Bp) relative to the hymen, in accordance with the Pelvic Organ Prolapse Quantification system (POP-Q). The grading system ranges from 0 (perfect muscle support) to 4 (complete vaginal inversion) (Ghetti, et al. 2005) (Weber and Richter 2005) (Bump, et al. 1996).

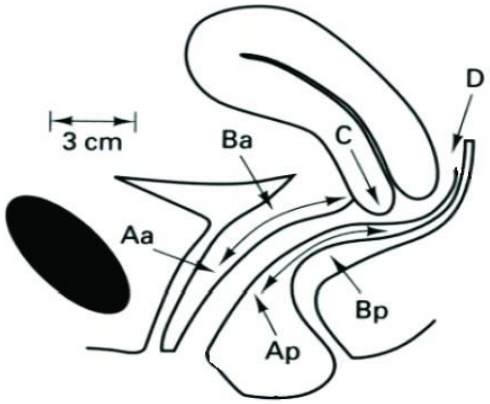

Figure 3: POP–Q system measurement points adapted from (Bump, et al. 1996)

2.3 POP Treatment

Generally, non-invasive treatments are recommended for the first-line management of PFDs.

POP may be treated surgically or non-surgically, depending on the severity of the condition.

Non-surgical treatment options for POP include pelvic floor physical therapy (PFPT), Kegel exercises, and pessary (Alas and Anger 2015).

Because damage to or relaxation of the PFMs leads to pelvic organ descent, it is critical to maintain proper muscle volume and closure of the LH. For this end, PFPT has shown a significant improvement in the symptoms of POP, more so than lifestyle modifications, pamphlets, or self-taught Kegels. PFM training is shown to increase muscle volume, shorten the muscle length, constrict the LH, lift the bladder neck and rectal ampulla, and overall improve stages 1, 2 and 3 of POP short term (Alas and Anger 2015) (Bø 2012).

Pessaries are soft devices mostly made of silicon that are considered a minimal intervention form of treatment used by 86% of gyneacologists and 98% of urogynaecologists in their practices. They come in various shapes and sizes which must be fitted to the patient according to their needs and are divided into two main categories: support pessaries (ring, lever, Gehrung, incontinence ring, Marland) and space-filling pessaries (Gellhorn, donut, cube) (Jelovsek, Maher and Barber 2007) (Alas and Anger 2015) (Lamers, Broekman and Milani 2011).

Despite reports that over 85% of fittings are successful, many patients abandon use due to discomfort or expulsions from incorrect fitting. It is also a less desirable option for young physically active patients (Alas and Anger 2015) (Lamers, Broekman and Milani 2011).

Although there are side effects associated with the use of pessary devices, most of them occur due to a lack of periodic doctor appointments. Patients using pessary devices saw improvement to their symptoms of POP short term, high reported satisfaction rates medium-term and an improvement to body image. The results of pessary use have been reportedly comparable to those of POP surgery in terms of quality-of-life improvement (Jelovsek, Maher and Barber 2007) (Lamers, Broekman and Milani 2011).

Surgical treatment

Surgical treatment of POP falls into two categories: reconstructive and obliterative. The first category is further divided into native tissue (NT) repair and mesh augmented (MA) repair. Repair techniques can be done using native tissue (native tissue primary repair) or mesh (reinforcement or overlay). (Jelovsek, Maher and Barber 2007) (Stanford, Cassidenti and Moen 2012).

There is a relatively high failure rate for POP surgery with the reappearance or new developments of POP in different compartments of the pelvic floor. A study by Olsen, *et al.* (1997) found that of 395 women who underwent POP and urinary incontinence surgery in 1995, 29.2% were undergoing repeat procedures. Some common complications of MA repair reported to the US Food and Drug Administration include erosion through vaginal epithelium, infection, pain, urinary problems, and recurrence of prolapse and/or incontinence (Daneshgari, Kong and Swartz 2008).

3 POP assessment

POP diagnosis and its treatment remains a relevant and scientifically challenging topic. In this chapter, currently existing and developing methods of assessing POP are exposed as well as their respective advantages and disadvantages.

3.1 Clinical examination

Standard diagnosis of pelvic organ prolapse is conducted through a standard pelvic examination in dorsal lithotomy position (in the case of obvious protrusion when the patient strains), in standing position (in milder cases of vaginal wall and uterine prolapse), or in Sim's position (to identify the type of prolapse) (Bhadana 2020).

The patient may be required to perform different types of efforts during the examination to evaluate the prolapse under varying levels of strain. These must be detailed for the sake of describing the stage of POP, along with the position of the patient, the type of table or chair used, the type of instruments used, the contents of the bladder and rectum and the diagrams of custom devices used (Weber and Richter 2005).

The types of strain may include:

- Passive, in a relaxed position, performed in the absence of effort.
- Valsalva manoeuvre, where the patient is asked to fill her chest with air and push, which causes the contraction of both the pelvic muscles and the abdominal wall simultaneously. This allows the evaluation of the maximum vaginal pressure performed by the patient as well as the maximum protrusion of the prolapsed tissue.
- Coughing and other stressors have a similar effect to the Valsalva manoeuvre.
- Contraction requires the patient to apply continuous pressure over a period of time, which is repeated four times to evaluate the progression of the vaginal pressure in contraction and recovery. The ability to contract and relax the pelvic muscles selectively and the strength of the contraction are evaluated. The patient may also be asked to contract the muscles for a duration of 10 seconds to evaluate any variations in the strength of the contraction over time. However, the results from this examination may be misleading as patients can erroneously activate other muscles simultaneously.

Although heavy straining allows for a better evaluation of the stage of maximum prolapse, it is discouraged to do so as this very action is a risk factor for developing POP (Bø 2012).

Pelvic organ position is measured in centimetres in accordance with the POP-Q to determine the stage of prolapse. Because the POP-Q does not take into account asymmetries in the hernia, imaging techniques (which lack standardization) may be used to evaluate the prolapse in addition to other examinations. For that purpose, a speculum may be used to visualize the vaginal walls and cervix. Photography may be used in cases of prolapse in stage 2 or higher to document the evolution of the patient's condition. Certain types of prolapse may also be diagnosed through endoscopy. Other imaging procedures include ultrasound, contrast radiography and computed tomography and magnetic resonance imaging (Bhadana 2020) (Bump, et al. 1996).

3.2 Probes and other measurement devices

The mechanical properties of tissues vary considerably with structural changes to the tissue caused by physiological and pathological processes as well as previously implanted mesh grafts. Diagnosis through manual palpation results in varied interpretations and does not allow for detailed quantification of the properties of the pelvic floor. As such, it is not possible to archive the exact results for later comparison to analyze the detailed evolution of POP in a patient and so the physician must rely on memory (Egorov, Raalte and Sarvazyan 2010).

Thus, it is necessary to take objective quantitative anatomical and biomechanical measurements using a specialized device. In this section, different devices currently in development are analyzed to understand the advantages and disadvantages of these solutions.

Vaginal tactile imaging

Due to the changes to the properties of tissues previously discussed, the measurement of disturbances to the pressure pattern and the generation of stress imaging are effective ways of detecting and quantifying said processes (Egorov, Raalte and Sarvazyan 2010) (van Raalte and Egorov 2015).

The vaginal tactile imaging (VTI) probes requires a very high amount of pressure sensors (96 and 120), resulting in a high cost of manufacturing. On the other hand, the abundance and variety of sensors allow for the measurement of various parameters and the shape facilitates measurements from different angles. The probe may be moved to measure pressure in different points as well as rotated to provide circumferential measurements from the vaginal walls. This way asymmetries in the structural characteristics can be detected and quantified (Egorov, Raalte and Sarvazyan 2010) (van Raalte and Egorov 2015).

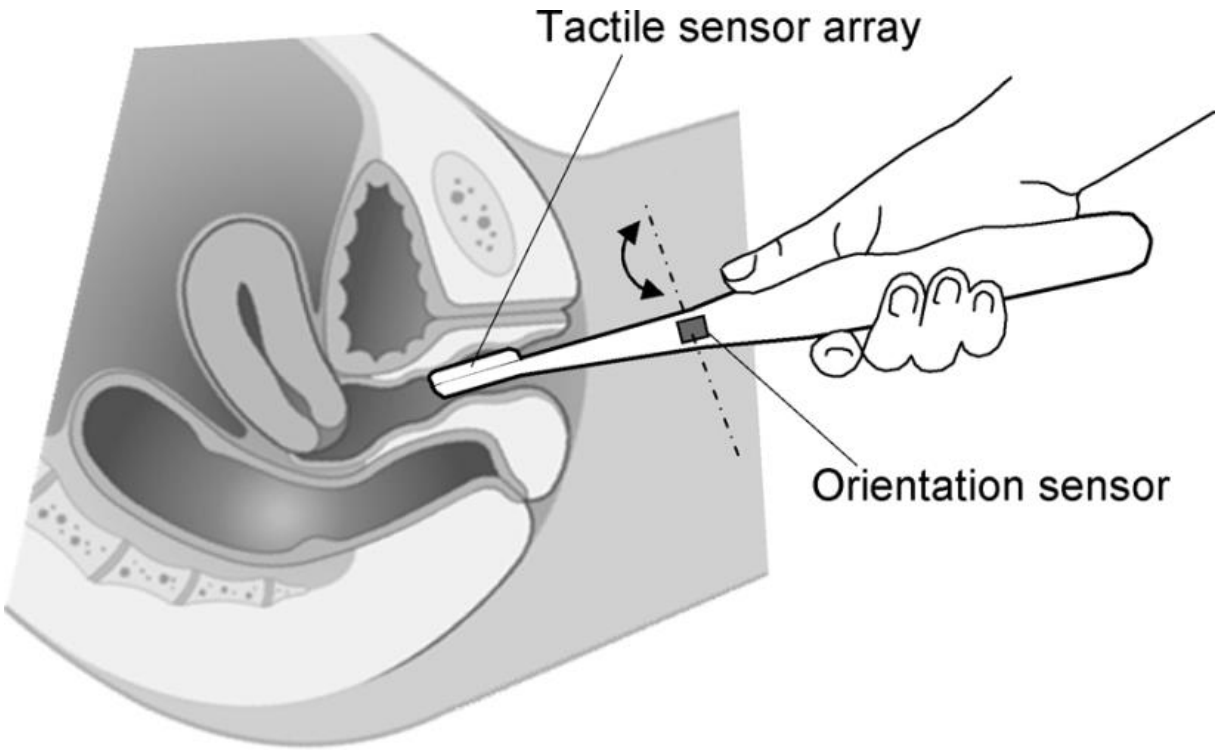

Figure 4: Tactile sensor array mounted on the tip of the VTI probe (Egorov, Raalte and Sarvazyan 2010)

Analysis using these devices demonstrated a higher degree of comfort when compared to manual palpation (54% of patients reporting more comfort) and the possibility of a very quick diagnosis. However, because the samples used in these studies were limited (22 and 13 women respectively), it is not certain that these devices with fixed shape and sizes will be usable for diagnosis to most patients (Egorov, Raalte and Sarvazyan 2010) (van Raalte and Egorov 2015).

The devices tested in these studies do not include machine learning algorithms which would allow for automatic diagnosis. As such, the physician must analyse the results and interpret numerical data which, in turn, may require professionals to receive specialized training.

Manometry-catheter

The vaginal manometer was originally created by Kegel as a form of biofeedback for patients during Kegel exercises. This first manometer, called perineometer, used a pneumatic resistance chamber which allowed to circumvent the issue of misleading measurements obtained from incorrect muscle activation through observation of its movement. The perineometers show similar results to manual palpation and ultrasound exams but inconsistency between perineometers of different manufacturers likely due to differences in resistance chamber sizes and materials. This device is also unreliable when used in patients with different anatomical characteristics due to the flexibility of the probe. Because the resistance chamber is 8cm long and is not moved during examination, it cannot determine the full pressure profile of the vagina but an average measurement between the main points (Cacciari and Sacco 2019) (Guaderrama, et al. 2005).

As such, a more reliable alternative was tested, withdrawing a four-channel water-perfused catheter at a constant speed of 8mm/s to acquire a full pressure profile. This technique allows for a distinction between the pressure in different points of the vagina and for a quick examination. The choice of water perfused catheter allows for a measurement of absolute pressure unlike the perineometer. Although this device is more precise at measuring pressure in specific points of the vagina, its measurements are not reliable in the distal vagina where the side holes of the catheter meet the air and erroneously measure atmospheric pressure (Guaderrama, et al. 2005).

The motorized puller makes for an extra expense that other devices do not have, along with all equipment associated with water-perfused catheters. Its reduced number of sensors may not give an adequate analysis and, like the vaginal tactile imaging devices previously mentioned, there is no machine learning algorithm.

Optical-fiber sensor device

Two varieties of this device were developed which consist of bivalve speculums with arrays of optical-fiber sensors (7 sensors and 9 sensors respectively) with 10 mm spacing along each blade. The first version of the device as shown in Parkinson, *et al.* (2016) used a manually expanded bivalve speculum whilst the second version in Parkinson, *et al.* (2019) presented a probe with automated expansion of its two blades. These allowed for real time measuring of absolute pressures and pressure distribution along the full vaginal length. The sensors used allowed for high spatial resolution which decreased manual handling and allowed for more comfort for the patients.

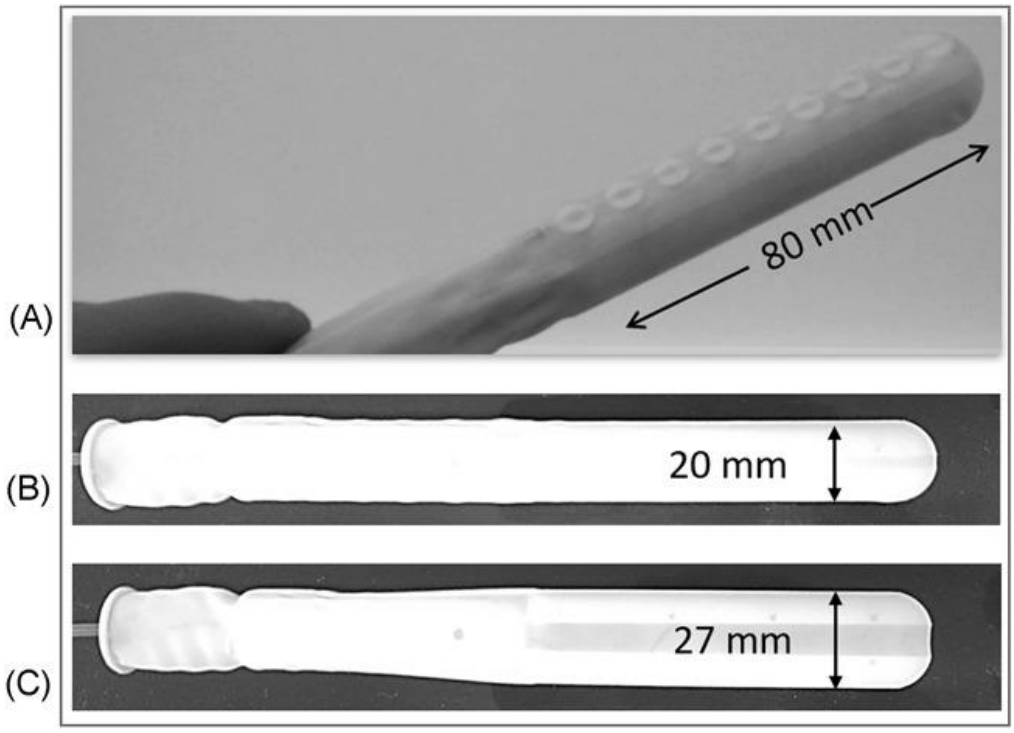

Figure 5: Optical-fiber probe; (A) showing sensors; (B) unexpanded sideview; (C) expanded sideview (Parkinson, Rosamilia, et al. 2019)

The high spatial resolution comes at the cost of a high number of fiber-optic pressure transducers which results in expensive manufacturing. These devices also bring handling difficulties due to the fragility of these types of sensors. The first version of the device required manual expansion which introduced user-dependent variables due to the dependence of the results on the pressure applied.

3.3 Conclusion

Current manual examination methods can't reliably evaluate and quantify the development of POP over time and known measurement devices are not currently available on the market. The device prototypes explored on the previous section present many disadvantages that make widespread use difficult, such as high production cost due to the amount of sensors and other unique device requirements, possible discomfort to the patients on account of the fixed shape of the probes, unreliable measurements, lack of data acquisition software or machine learning models that would allow for an easy interpretation of the results by the physician and to analyse the progression of the condition. Diagnostic methods which rely on conscious strain by the patient result in varying effects of intraabdominal pressure (IAP) as different muscles may be activated which may not allow for an accurate measurement of the properties of the vaginal wall. Continuous straining during examinations may even worsen the condition in some cases.

The development of the device presented by this work aims to create a reliable, affordable, and easy to use method of diagnosis for POP in early stages. This early diagnosis is essential to possibly recommend conservative treatment and thus prevent the worsening of the condition, improving quality-of-life for the patients and reducing the costs and complications associated with surgery.

This device must have lower production costs to make it a viable purchase by clinicians and therefore become part of a standard diagnosis. This way any subjectivity between diagnostics can be cleared. It must also be intuitive to use to avoid requiring special extra training for the clinicians, as well as provide easy to interpret results through machine learning algorithms. To analyse the progression of the condition, data acquisition is necessary, and it must be possible to keep a track record of each patient. This is essential to apply the correct treatment, evaluate the current treatment's effectiveness and therefore prevent further aggravation. It must be portable, reusable, and easy to clean and sterilize. It is also important for the diagnostic tool to allow for passive testing to prevent a dependence on correct muscle activation by the patient and be able to collect data on different dilations to replace the need for strain. To avoid the user dependent factors found in Parkinson, *et al.* (2016), these dilations must be done at exact increments and measurements taken statically at each stage. The shape of the body of the device must be comfortable and minimally invasive for the patient.

4 Materials and methods

In this chapter, the device and its components are described, followed by the experimental protocol.

4.1 Concept

This work presents an early version of a device that aims at performing distributed pressure measurements along the anterior and posterior vaginal wall and collecting data in real-time to assess the condition of the patient to detect POP as early as possible, evaluate the stage of the condition and facilitate the choice of treatment. Because it is meant to measure anterior and posterior pressure profiles, it excludes the proximal wall and, therefore, cannot diagnose enterocele and uterine prolapse. The pressure range of the final device should be between 0 and 147 mmHg, the highest pressure reading found by Shaw, *et al.* (2014). For this work, readings are focused on relaxed tissues and the force range considered was up to 13 N, the instant maximum force found by Amorim, *et al.* (2017) with PFM contraction.

This device is meant to be used in a complete POP diagnosis by performing passive, contraction, and Valsalva examinations. It also aims to be used to diagnose urinary incontinence by evaluating how long a patient can hold a contraction and how the strength varies over time. To that end, it must record data over time and plot the evolution of load. It should also be used to evaluate improvements to a patient's pelvic floor muscles to determine the effects of any treatment in use or to detect possible adverse side effects of surgical interventions. The collection of clinical data with this device will provide data for a future machine learning algorithm that will be used for automatic diagnosis. This clinical data will also provide information on vaginal properties to be used in computational models to simulate the behaviour of the pelvic floor and evaluate POP correction techniques *in silico*.

In this work, tests were performed *ex vivo* and thus only allowed for passive testing. Using different dilations of the speculum in passive tests makes it possible to take objective measurements without relying on correct muscle activation and consistent application of force by the clinician.

The device works by taking static measurements at precise dilations; when the expansion of the instrument is achieved, the readings are collected during some time. In trials described ahead, force measurements will be taken with the device and with tensile tests, and higher force readings will correspond to higher elastic modulus associated with greater firmness of the materials.

4.2 Device development

Physical instrument

In place of a probe, a standard stainless steel bivalve speculum was used as the physical instrument. This instrument allows for a better fit adaptable to different patients for a more comfortable examination than a fixed shape probe. Because it is a standard medical instrument, production costs are reduced, and its use is more intuitive for the physician and the shape is ergonomic.

The speculum was modified by cutting slits on the upper and lower blades to place both FlexiForce sensors. The sensors must be connected to the development board (figure 6-F) through the inner side of the speculum (figure 6- C) near the adjustment screws (figure 6- E) to avoid obstruction to the user and have the sensing area (figure 6- B) on the outer side of the

blades (figure 6- A) where the measurements are taken. The speculum and FlexiForce OEM Development Kits were mounted on a previously made 3D printed base piece (figure 7), requiring the user to hold a handle with one hand and adjust the opening of the speculum with the other.

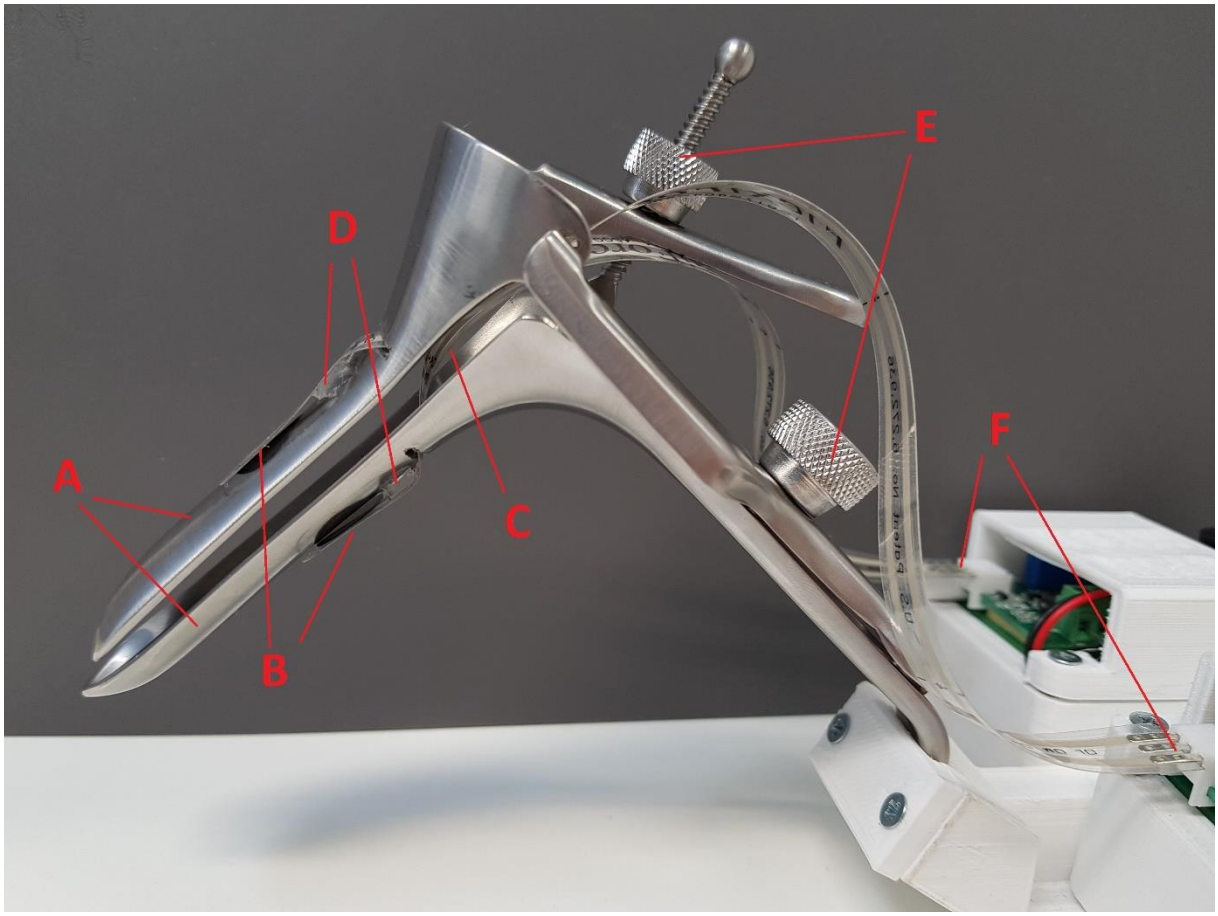

Figure 6: Assembled device: A- outer side of the speculum blades; B- sensors' sensing area; C- inner side of the speculum blades; D- polyurethane double-sided tape; E- adjustment screws; F- sensor connection to QuickStart circuit board

Figure 7: Device base piece with the two development boards

Development board

Two FlexiForce OEM Development Kits were used, one for each of the two sensors placed on each speculum blade. It includes a development board, sensors, USB cables, and software. The development board (figure 8) is made up of an Arduino module (MicroView USB interface board and controller with OLED display), a start-up and a tare button, the QuickStart circuit board with a potentiometer, pluggable terminal block, a 3-pin sensor connector, an attached 9-volt battery clip. The Arduino module converts the analogue signal from the QuickStart circuit board into a digital signal which is outputted into the software output window and the OLED display. The system was powered using 3 m long USB cables connected from the USB cable connector (figure 8- 3) to the computer for an input voltage of 5V (©Tekscan Inc. 2018).

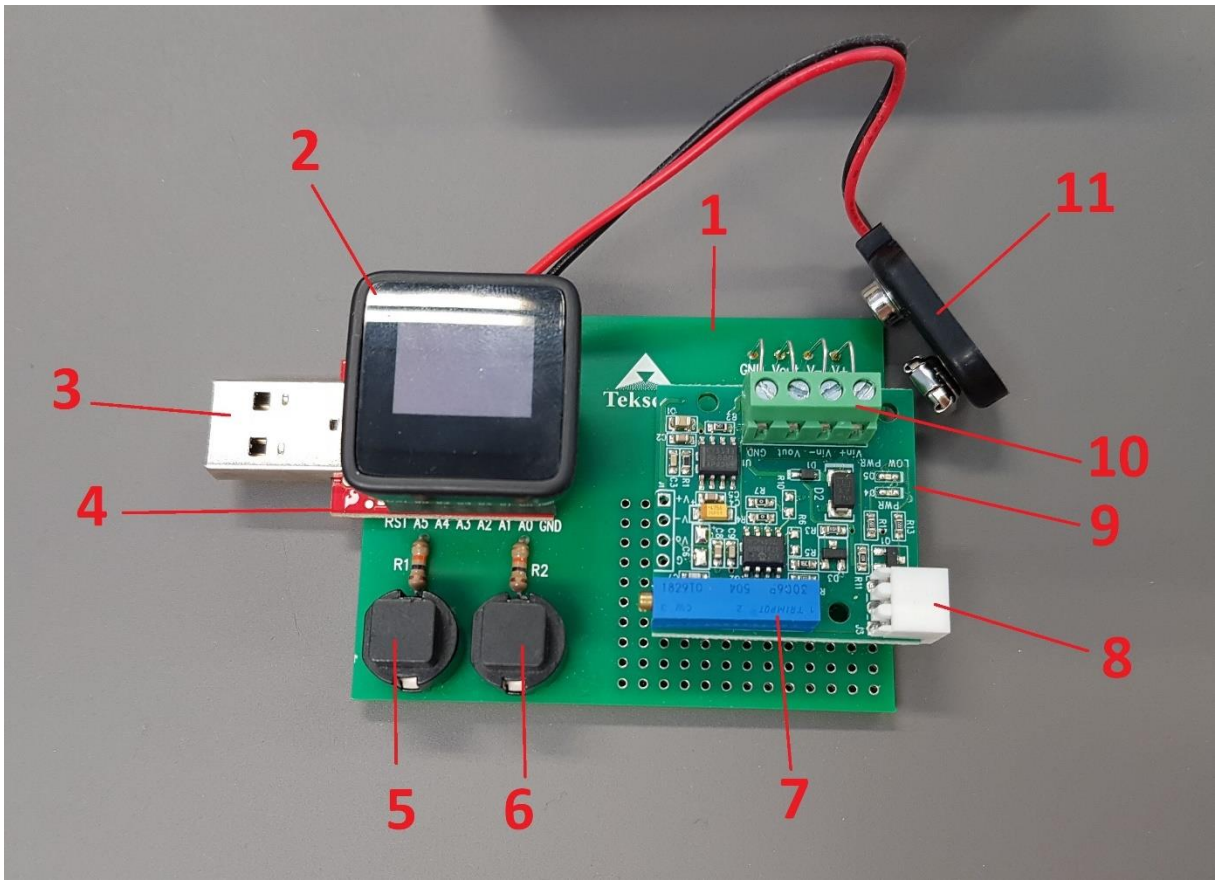

Figure 8: OEM development board: 1- development board; 2- MicroView controller with OLED display; 3- USB cable connector; 4- MicroView USB interface board; 5- Tare button; 6- Start-up button; 7- R9 Potentiometer; 8- 3-pin sensor connector; 9- QuickStart circuit board; 10- Pluggable terminal block; 11- 9V battery clip

Sensors

For this development stage, two standard force sensors were used, which allow for lower costs and the fulfilment of preliminary demands. The sensors used were the standard FlexiForce A201 sensors (figure 9) which are ideal for prototyping and proof of concept. The length of 191 mm allows the speculum to be fully opened, and the 14 mm width is smaller than the blades. It is non-intrusive thanks to the 0.203 mm thickness, and its flexibility allows it to adapt to the shape of the speculum and its irregular openings. These sensors measure a contact force derived from the compliance of surfaces. The sensor placed on the upper blade is meant to measure anterior forces, and the sensor is placed on the lower blade's posterior forces (©Tekscan Inc. 2021).

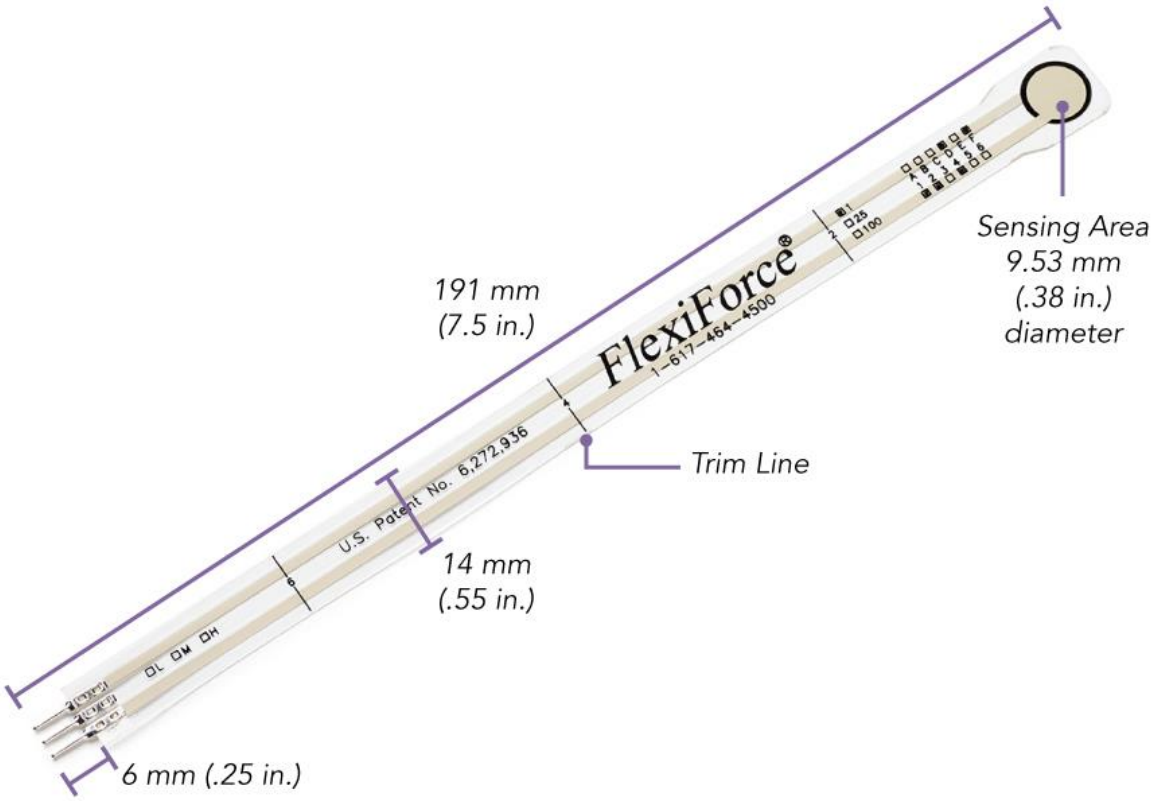

Figure 9: FlexiForce A201 Sensor (©Tekscan Inc. 2021)

Two standard force sensors were used with different standard force ranges: 4.4 N (labelled as sensitivity 1) and 111 N (labelled as sensitivity 25). These ranges can be adjusted by changing the value of the feedback resistor through the potentiometer. For this purpose, a 100 kΩ resistor was inserted in the sensor connector's two outer pins, and a jeweller's screwdriver was used to adjust the potentiometer to the desired value (as illustrated in figure 10). Higher feedback resistance is resulting in a lower force range and vice-versa. For this work, different combinations of sensors and feedback values were tested. As the Arduino module's digital output is 10-bit (corresponding to $2^{10} = 1024$ steps) and the input range is 0-5V, the system resolution is 4883µV per A/D count.The sensors come at a resolution of 19531µV per A/D count (©Tekscan Inc. 2018) (©Tekscan Inc. 2021).

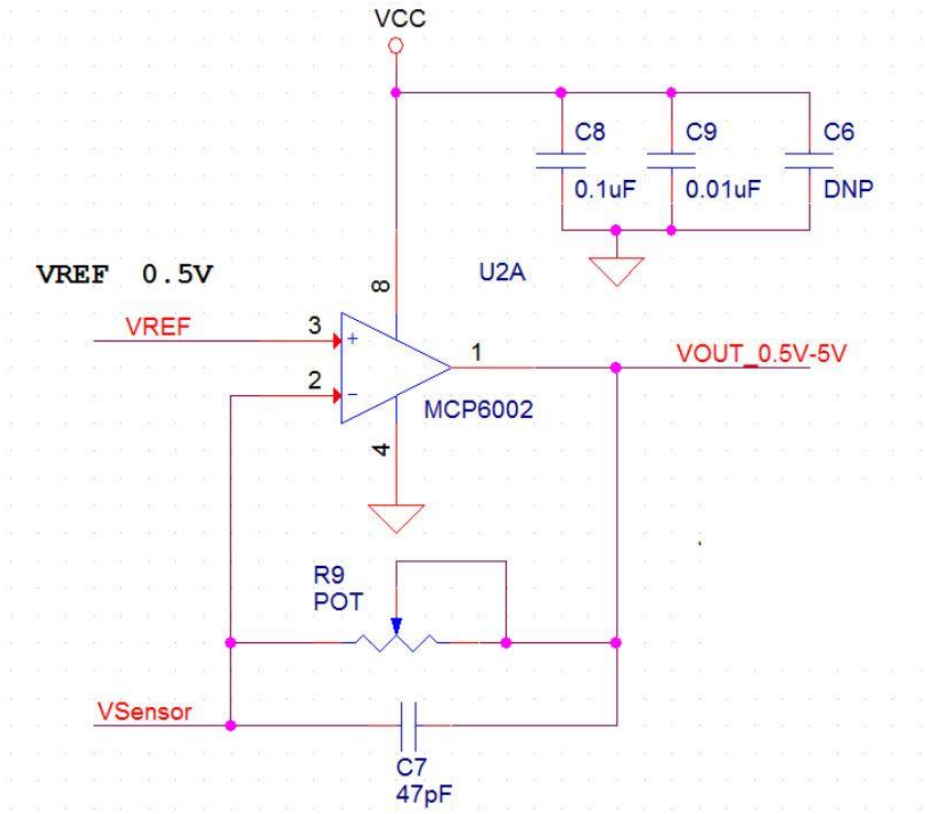

Figure 10: Signal conditioning circuit, where VOUT=VREF×(1+R9/Rsensor) (©Tekscan Inc. 2018)

Polyurethane double-sided tape was used to attach the sensors to the outer sides of the speculum blades. A strong enough hold was necessary to ensure consistent results, but the material must be easy enough to remove for sanitization, disassembly, or part replacement. The tape was placed outside the sensing area to avoid interfering with the measurements due to its 2mm thickness, but close enough to prevent movement of the sensors.

Data acquisition

The FlexiForce Microview software has a data acquisition rate of 10 Hz and displays both instant readings and output by sample number graph (figure 11). The default Arduino code was kept, but a new excel Microview reader was made to view both sensors' recorded readings simultaneously (figure 12) (©Tekscan Inc. 2018).

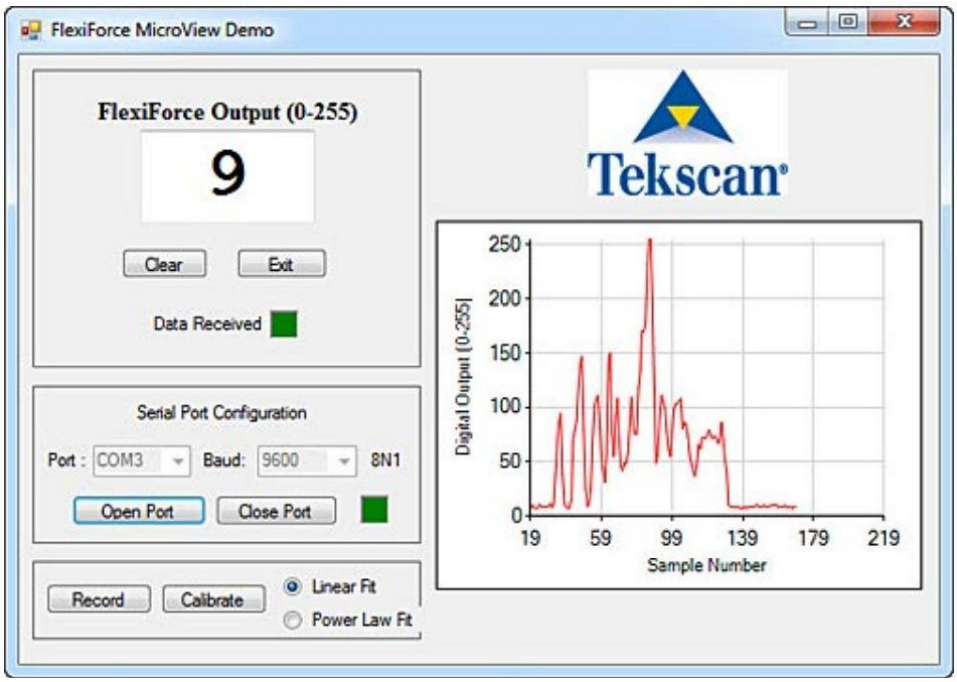

Figure 11: FlexiForce Microview interface with uncalibrated instant reading (top left corner) and readings plotted over time (right) (©Tekscan Inc. 2018)

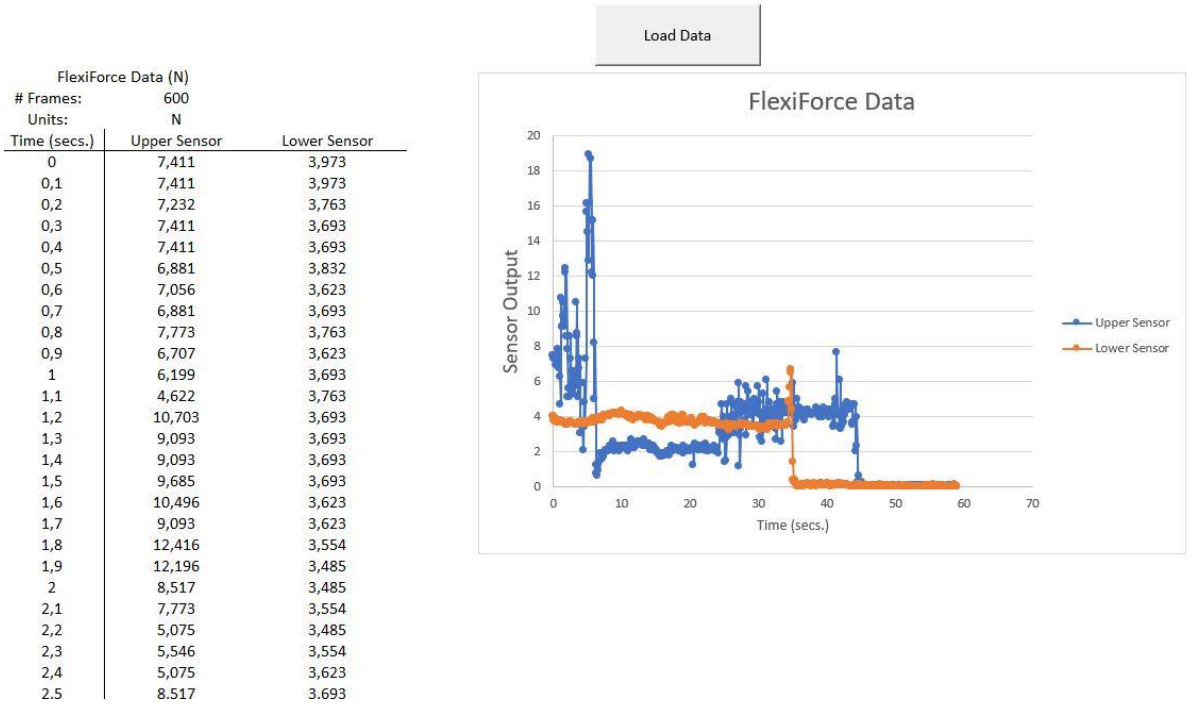

FlexiForce Data (N)

# Frames:	600	
Units:	N	
Time (secs.)	Upper Sensor	Lower Sensor
0	7,411	3,973
0,1	7,411	3,973
0,2	7,232	3,763
0,3	7,411	3,693
0,4	7,411	3,693
0,5	6,881	3,832
0,6	7,056	3,623
0,7	6,881	3,693
0,8	7,773	3,763
0,9	6,707	3,623
1	6,199	3,693
1,1	4,622	3,763
1,2	10,703	3,693
1,3	9,093	3,693
1,4	9,093	3,693
1,5	9,685	3,693
1,6	10,496	3,623
1,7	9,093	3,623
1,8	12,416	3,554
1,9	12,196	3,485
2	8,517	3,485
2,1	7,773	3,554
2,2	5,075	3,485
2,3	5,546	3,554
2,4	5,075	3,623
2.5	8.517	3.693

Figure 12: Excel Microview reader adapted to two simultaneous sensors

4.3 Calibration

The sensors used in this device require calibration before each testing cycle, so it was necessary to determine the best method to build an experimental procedure. Several calibrations were performed for each calibration protocol, and the raw calibration values were registered. These raw values correspond to a digital output by the sensors. The OEM development kit offers two calibration methods, linear fit and power-law fit, both considered and tested for this work's application (©Tekscan Inc. 2018).

Before calibration, OEM Development Kit was powered by the computer using the USB extension cables. The FlexiForce Microview software was opened twice, selecting the USB port for each OEM development kit. The startup button was pressed, followed by the tare button. Calibration was performed for each sensor in its own Microview window simultaneously.

For different calibration protocols (presented in table 1), the force range was adjusted by changing the value of the feedback resistor through the potentiometer depending on the samples used in the tests.

Linear fit calibration requires the application of known fixed loads to the sensor to draw a straight line from the calibration points. To use this calibration, three loads were applied directly to the center of the sensors while resting on a flat surface. In the prompt window, three calibration points were selected, and the unit was specified as Newton. A 1€ coin and two small weights were used with respective weights of 7.44 g, 19.705 g and 49.305 g, corresponding to the calibration point values of 7.2912 N, 19.3109 N and 48.3189 N (calibration *a* on table 1). For each point, the force value was entered into the dialog window and the weight was placed at the center of the sensor. A few seconds are waited for the values read by the sensor to stabilize, after which the OK button was pressed, and a raw value was displayed. This process was repeated for each weight, and the raw values were registered. This procedure is summarized in the following flowchart.

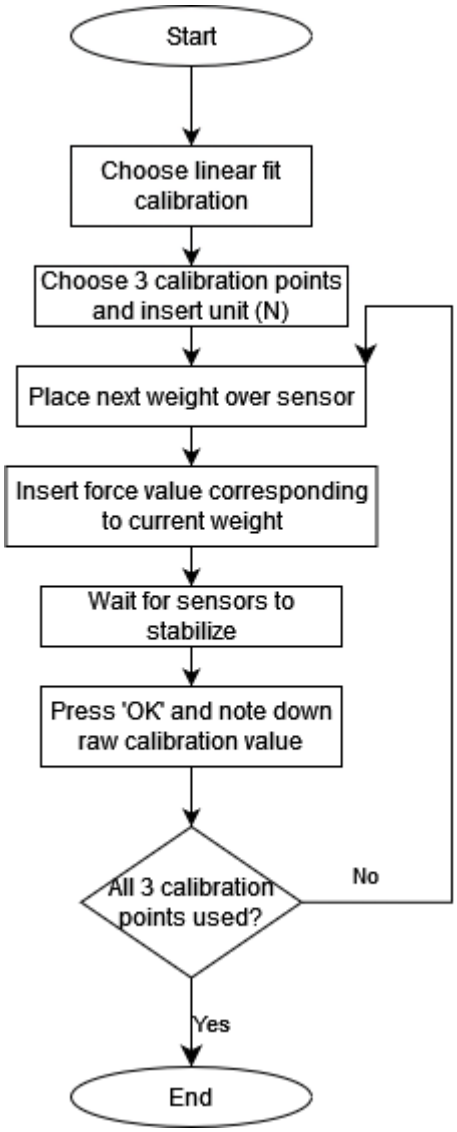

Figure 13: Linear fit calibration procedure summary flowchart

Power-law fit calibration calculates a power-law equation (as shown below) based on three load distribution values.

$$y = a \times x^b$$

Y corresponds to the force value and *x* to the raw digital output resulting from said load, with *a* and *b* calculated from the calibration points. The 3 calibration points used should correspond to 30%, 60% and 90% respectively of the total experimental load expected. For this work, the experimental loads are the loads measured in each speculum dilation. As such, calibration was made using the same speculum dilations. To this end, a sample was cut from a glove finger (procedure described in the next section) and put through a uniaxial force tensile test where the points corresponding to the speculum openings were used as the three calibration values. The device was fully assembled, and the calibration sample was placed on the speculum over the sensors. Each calibration point (1, 2 and 3) corresponds to a speculum dilation (17 mm, 26 mm, 35 mm), which allows for a calibration consistent with the practical use of the instrument. The Newton unit was entered into the dialog window, followed by the first calibration point value. The speculum blades were adjusted to a parallel position with a 17 mm opening between the outer sides of the speculum where the sensors are placed. After the output values stabilized, the OK button was pressed, and a raw value was generated and displayed. The value of the next calibration point was entered, and the blades were then kept in a horizontal position and opened

to a 26mm dilation. The rest of the process was repeated for this opening and the largest 35mm opening using the second and third calibration points, and all raw values were registered. This procedure is summarized in the following flowchart.

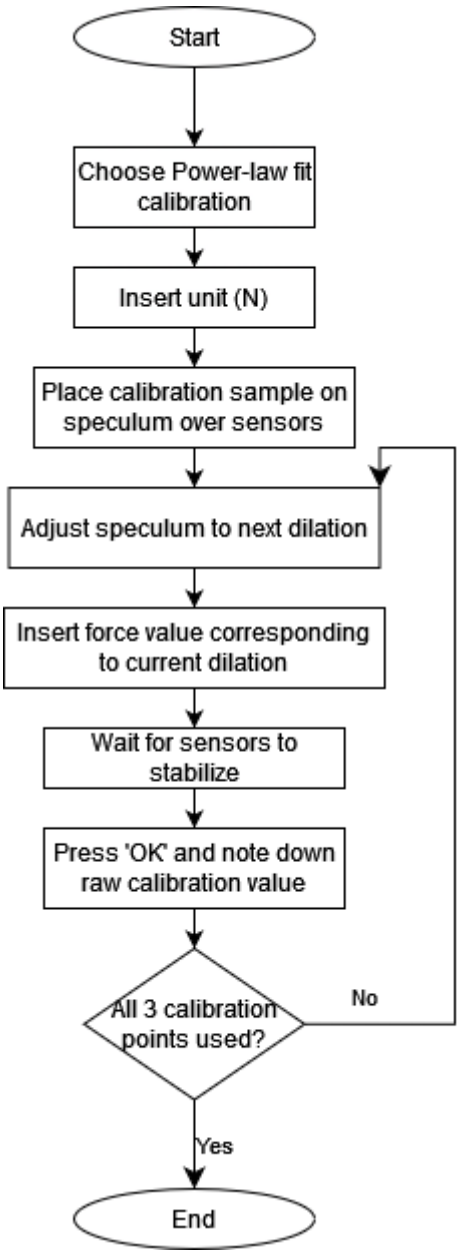

Figure 14: Power-law fit calibration procedure summary flowchart

Table 1: Calibration protocols used

Calibration type	Calibration protocol	Sensor	Potentiometer adjustment	Sample used	Calibration Point	Speculum Dilation (mm)	Force value (N)
Linear fit	a	sensitivity 1	250	weights	1		7,2912
					2		19,3109
					3		48,3189
Power-law fit	b	sensitivity 1	250	1	1	17	0,02
					2	26	0,8
					3	35	2,48
	c	sensitivity 25	250	12	1	17	0,26
					2	26	5,92
					3	35	8,96
	d	sensitivity 1	50	12	1	17	0,26
					2	26	5,92
					3	35	8,96
	e	sensitivity 1	150	12	1	17	0,26
					2	26	5,92
					3	35	8,96

4.4 Glove finger testing

An initial form of testing was used to prepare the device to perform *ex vivo* testing and to create the best procedure, making use of glove fingers. This choice is due to the ease of acquiring a high number of samples and the shape and material characteristics being compatible with the dimensions of the device and the range of the sensors. The elasticity of the glove materials and the reduced size of the dilations allowed for multiple test cycles without concerns for changes to samples' properties. Three types of gloves were used, two types of latex and one type of nitrile rubber. Both types of sensors were also used to determine which is more practical for the application.

A pair of tensile test pieces were produced, using additive manufacturing to mimic the approximate shape of the speculum blades. These were mounted on the tensile test machine to hold the samples for testing, as shown in figure 15.

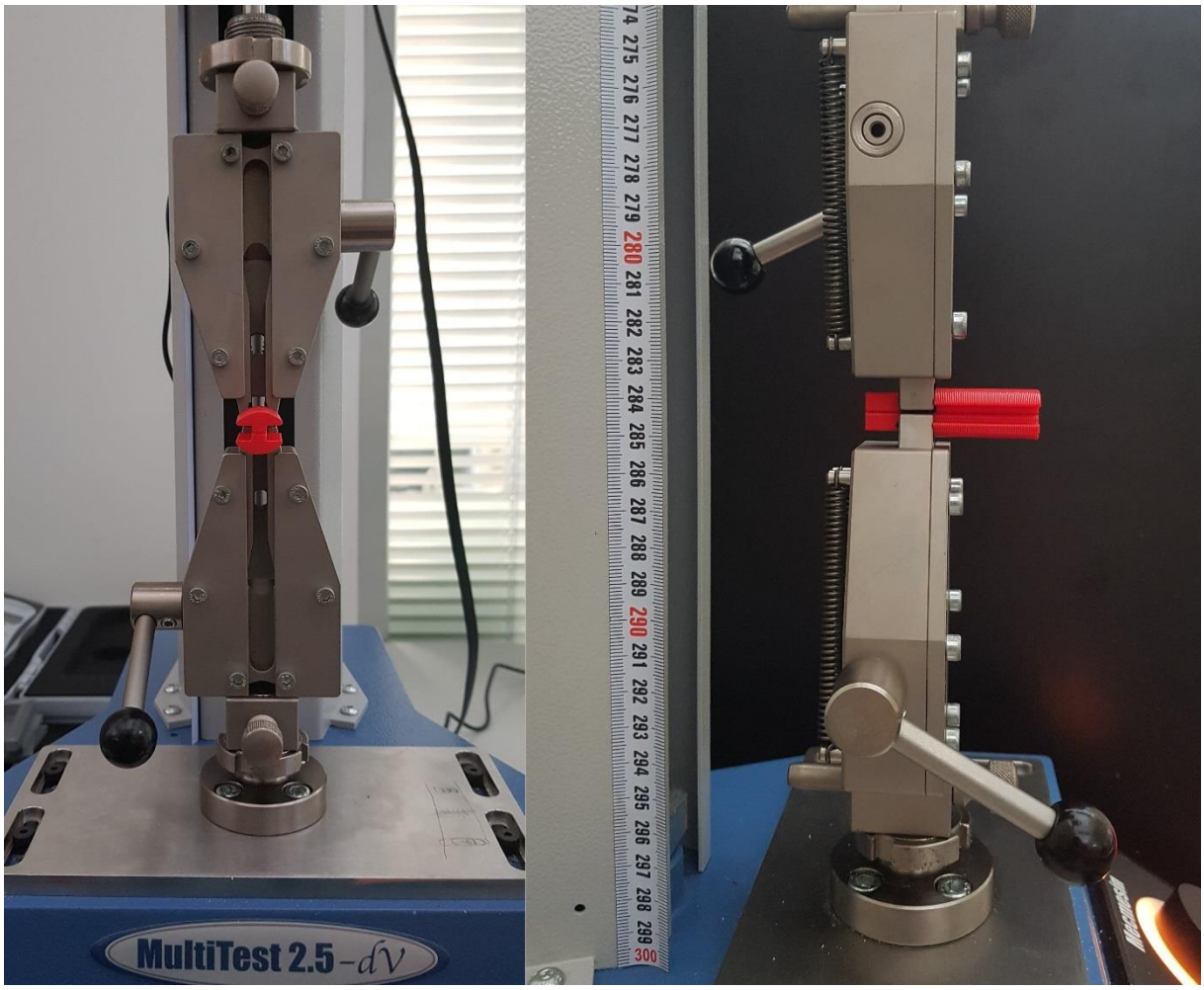

Figure 15: Tensile test pieces mounted in fully closed position on the tensile test system with a 100 N force gauge

The glove fingers were cut into samples with a scalpel and surgical scissors perpendicularly to the longitudinal axis under 30mm long and over 18mm to fit into the speculum-shaped tensile test pieces, as shown in figure 16. Different fingers were used to test different diameters, and care was taken to avoid samples with a great difference in diameter on each side. Variety in diameters and differences in materials allow testing the way the device reacts to different force ranges.

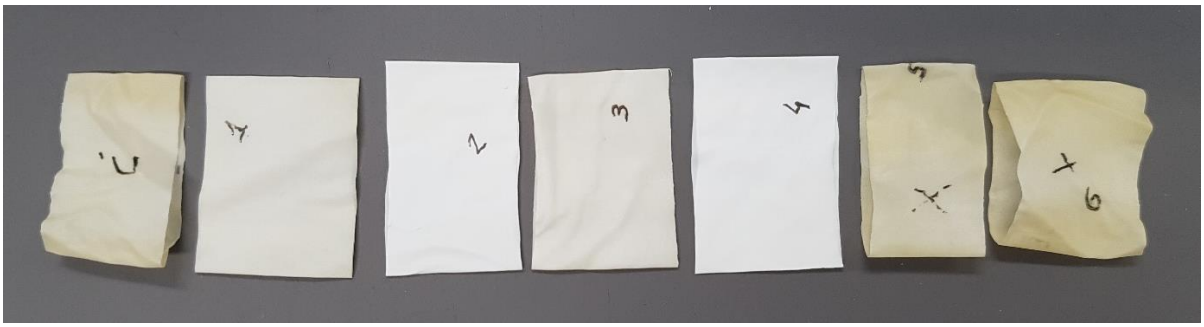

Figure 16: Latex glove samples

The sensors were calibrated using both methods for the latex samples and the power-law fit calibration for the nitrile rubber samples. Each sample was placed on the speculum and over the sensors and the device was opened from the closed position to one of 3 opening options and left unmoved to record the measurements. The dilation values were 17, 26 and 35 mm between the outer sides of the speculum where the sensors are placed. The speculum blades start completely closed and are placed in a horizontal position to reach the first opening and are then left horizontal for all dilations, only altering the vertical distance in between. The results of the upper and lower sensors are registered in excel spreadsheets for later comparison.

The force tensile test machine was equipped with the 100 N force gauge and the test pieces where the samples are placed (figure 17). It was first programmed to perform a static load test for each sample at an elongation rate of 1 mm/s to a maximum distance of 18 mm (corresponding to the maximum dilation of 35 mm) and a starting distance between test pieces of 3 mm (corresponding to the minimum dilation of 17 mm). For testing the nitrile samples, it was then decided to opt for separate dilation tests, where each sample was elongated at a rate of 1 mm/s from the closed position to the first opening of 3 mm (corresponding to the lowest dilation of 17 mm), then from this distance to 12 mm (intermediate dilation of 26 mm) and lastly to 21 mm (maximum dilation of 35 mm).

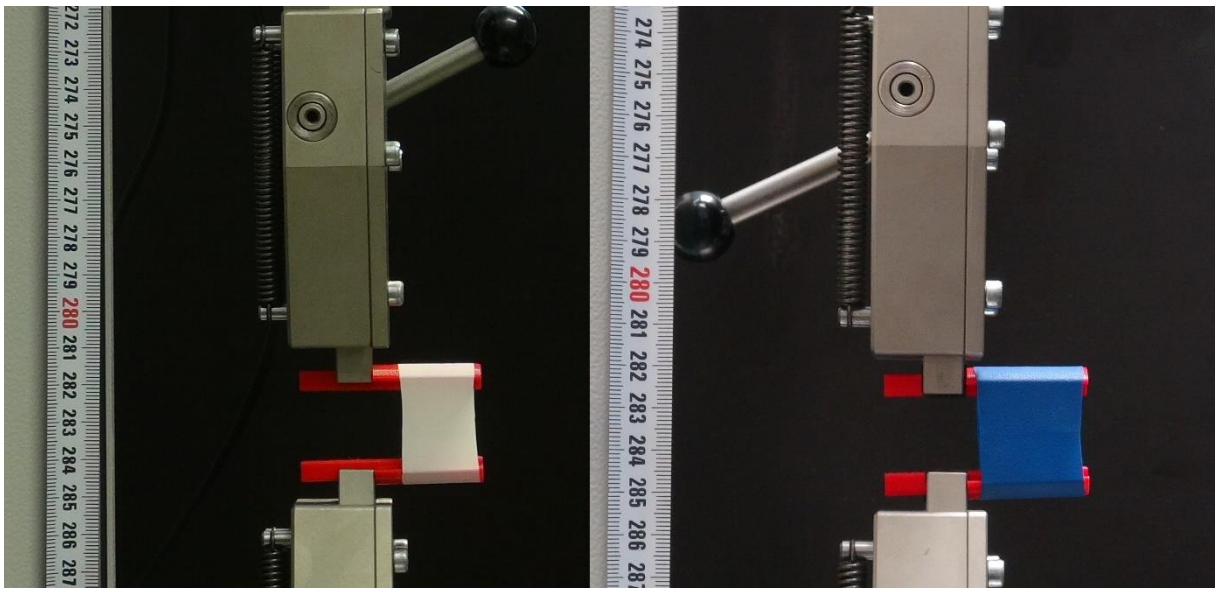

Figure 17: Tensile test of latex (left) and nitrile (right) samples at maximum opening

4.5 *Ex vivo* testing

Ethics Issue: Along the pipeline to clinical testing, animal models are typically used. This project involves experimentation with animal vaginal tissues. All the tissues animal testing procedures will be in conformity with the Directive 2010/63/EU of the European Parliament and the Portuguese DL 113/2013. All procedures were approved by the Ethics Committee and the Veterinary Authorities of Portugal (DGAV). The experimental procedures with animal tissues were performed according to the "Guidance Document on the Recognition, Assessment and Use of Clinical Signs as Humane Endpoints for Experimental Animals Used in Safety Evaluation" by OCDE (2000).

For *ex vivo* testing, three excised pork vaginas were used (figure 18-A). The vaginal wall was cut into samples with a scalpel and surgical scissors perpendicularly to the longitudinal axis under 30 mm long and over 18 mm (figure 18-B) to fit into the speculum-shaped force tensile test pieces. The probe sensors were calibrated using glove finger sample 12 with power-law fit calibration. Because the tissue properties are subject to change with time and strain, each sample could only be put through one test cycle each. A total of eleven samples were prepared and numbered from 1 (distal vagina, closest to the vulva) to 3 or 4 (proximal vagina, closest to the cervix).

Figure 18: Pelvic floor 1 (A); samples 1-1 through 1-4 (B), from left to right

Each specimen was placed on the speculum protected by a female condom (figure 19) which was opened from the closed position to one of 3 opening options and left unmoved to measure 600 data points over 1 minute. The dilation values were 17, 26 and 35mm between the outer sides of the speculum where the sensors are placed. The speculum blades start completely closed and are placed in a horizontal position to reach the first opening and are then left horizontal for all dilations, only altering the vertical distance in between. The results of the upper and lower sensors are registered in excel spreadsheets for later comparison. In cases where it was impossible to open the speculum to 25 or 35mm due to limitations in the tissue elasticity, a smaller in between opening was used and specified.

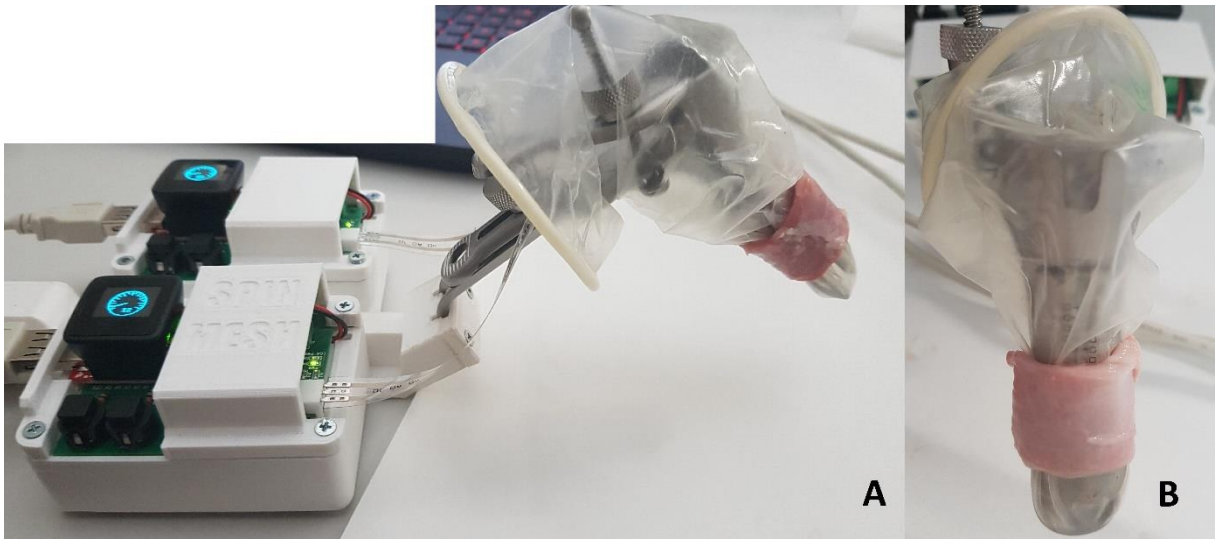

Figure 19: *Ex vivo* samples placed on the speculum with a 17 mm dilation over the sensors protected by a female condom; side view (A); top view (B)

The same pair of tensile test pieces was used for these tests (figure 20). The tensile test machine *Mutitest 2.5 dV* was equipped with the 100 N force gauge and programmed to perform three static load tests for each sample at an elongation rate of 0.8 mm/s and maintain that opening for 60 seconds. This waiting time is meant to replicate the relaxation of tissues between each speculum dilation in the device tests. Each test with a respective opening of 3, 12 and 21mm to account for the size of the testing pieces. These openings were subject to adjustments depending on which opening was used on the samples in the probe tests.

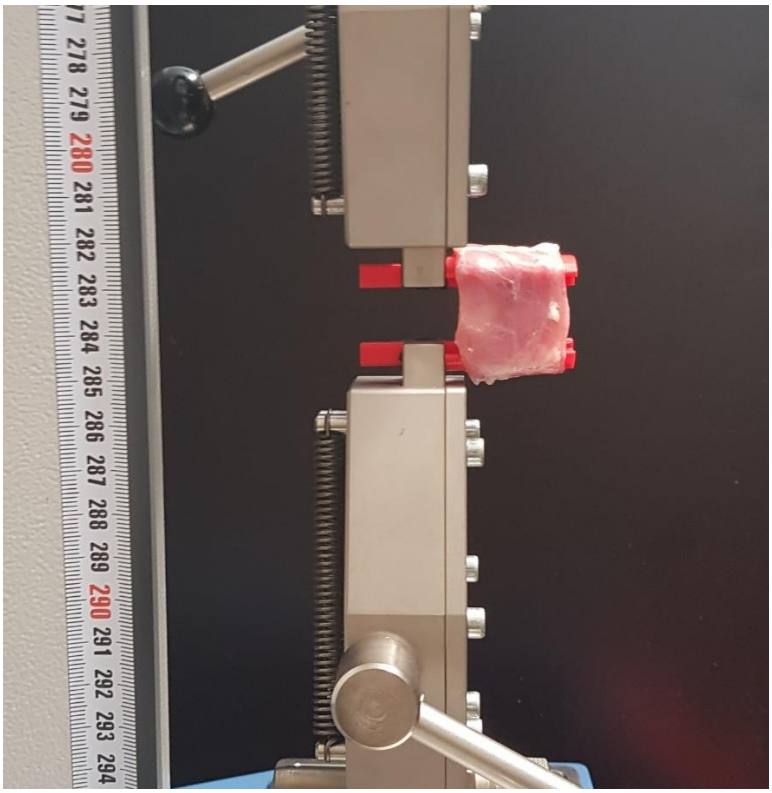

Figure 20: Tensile test of *ex vivo* sample at maximum opening

Each uniaxial test was performed immediately after the probe tests to prevent excessive drying and relaxation of the sample tissues and therefore obtain more precise results.

5 Results

This chapter presents experimental data and its analysis.

5.1 Calibration results

The linear fit calibration method was not used in most tests because it fails to account for the materials' compliance and the distribution of loads on the sensors. Another issue was that despite using the highest sensitivity sensors adjusted to low force ranges, high loads were necessary to obtain readings that did not match the expected measurements of the samples. It also required the disassembly of the device to perform each calibration on a flat surface which adds complexity to the procedure and creates inconsistencies in the sensor placement with each testing cycle. On the other hand, power-law fit calibration allowed both to account for the material's compliance and made a calibration consistent with the practical use of the speculum.

Sample *c* was initially meant to be used to calibrate the latex glove tests but quickly proved to be unreliable due to its narrow width. For that reason, sample 1 was used instead (for calibration protocols *a* and *b*) but this proved to have been a wrong choice as its force range is too low compared to that of other latex samples, as shown in figure 21-Sample 1. For the nitrile tests, sample 12 was chosen as the calibration sample for its advantageous dimensions that allowed for quick and consistent placement on the speculum over the sensors, in conjunction with its maximum force obtained in tensile tests of 8.96 N (figure 21-Sample 12), which was high enough to cover the force range of the other nitrile samples and theoretically of *ex vivo* samples as well. Tensile test results are shown as force measured by the force gauge as a function of a travelled distance corresponding to the speculum dilation for ease of reading.

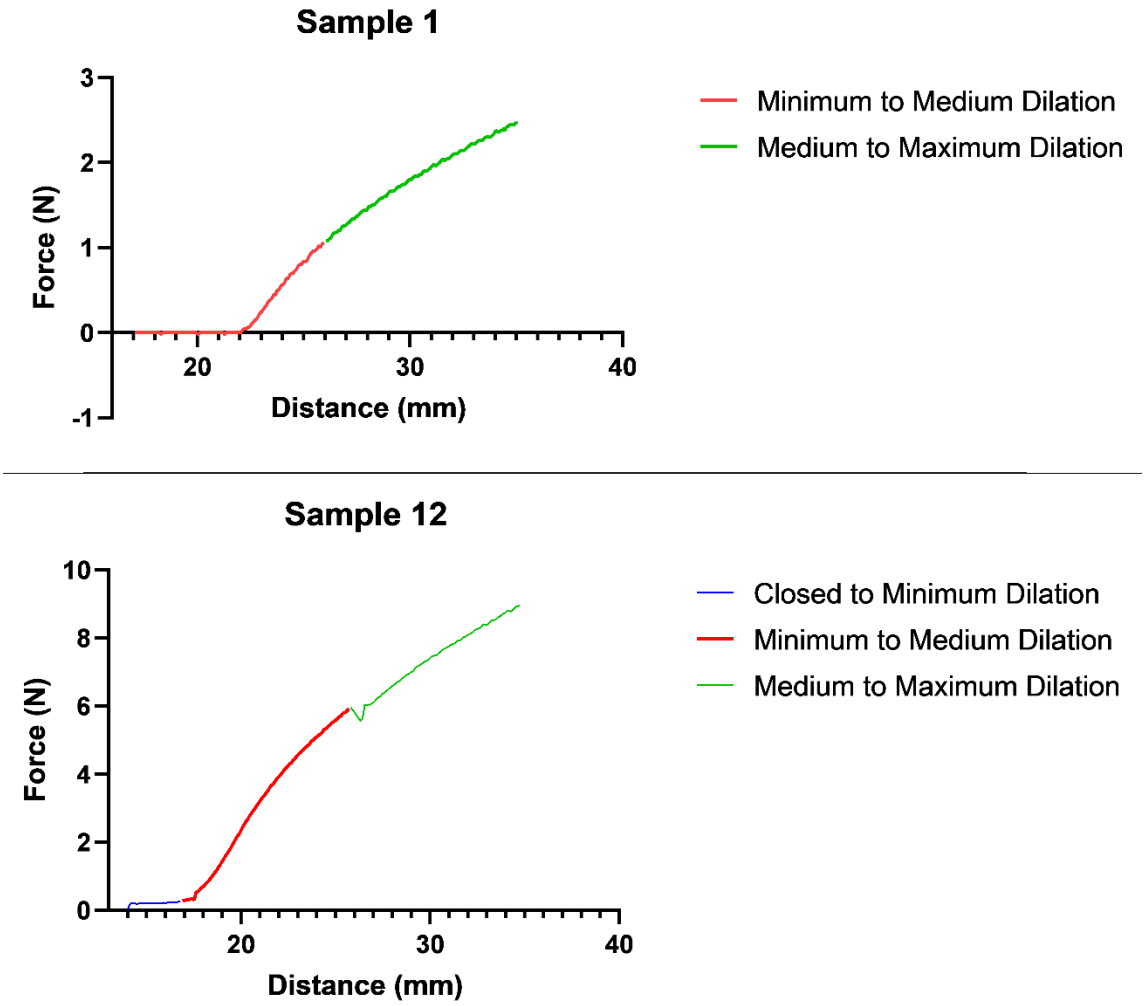

Figure 21: Tensile test results in load-distance curves for calibration sample 1 and 12, with Closed corresponding to the closed speculum position, Minimum dilation of 17 mm, Medium dilation of 26 mm and Maximum dilation of 35 mm

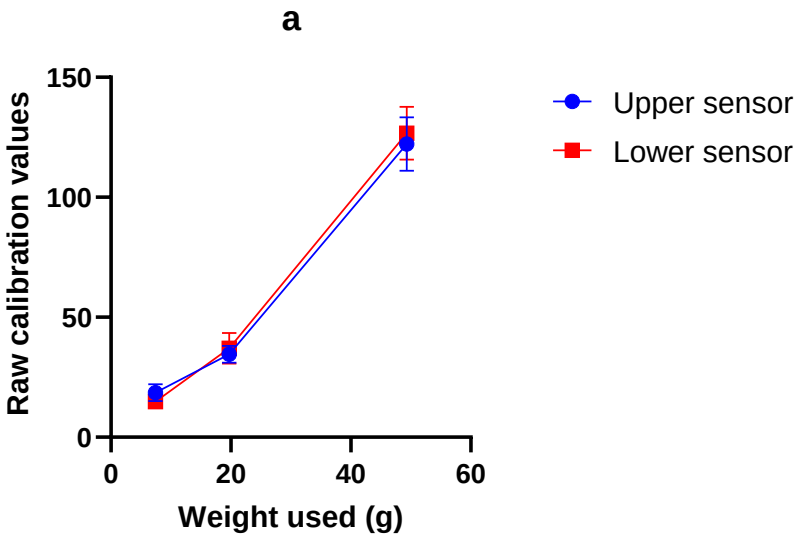

Figure 22: Mean raw values ± SEM (vertical axis) obtained in linear fit calibration (a) for each calibration point (horizontal axis)

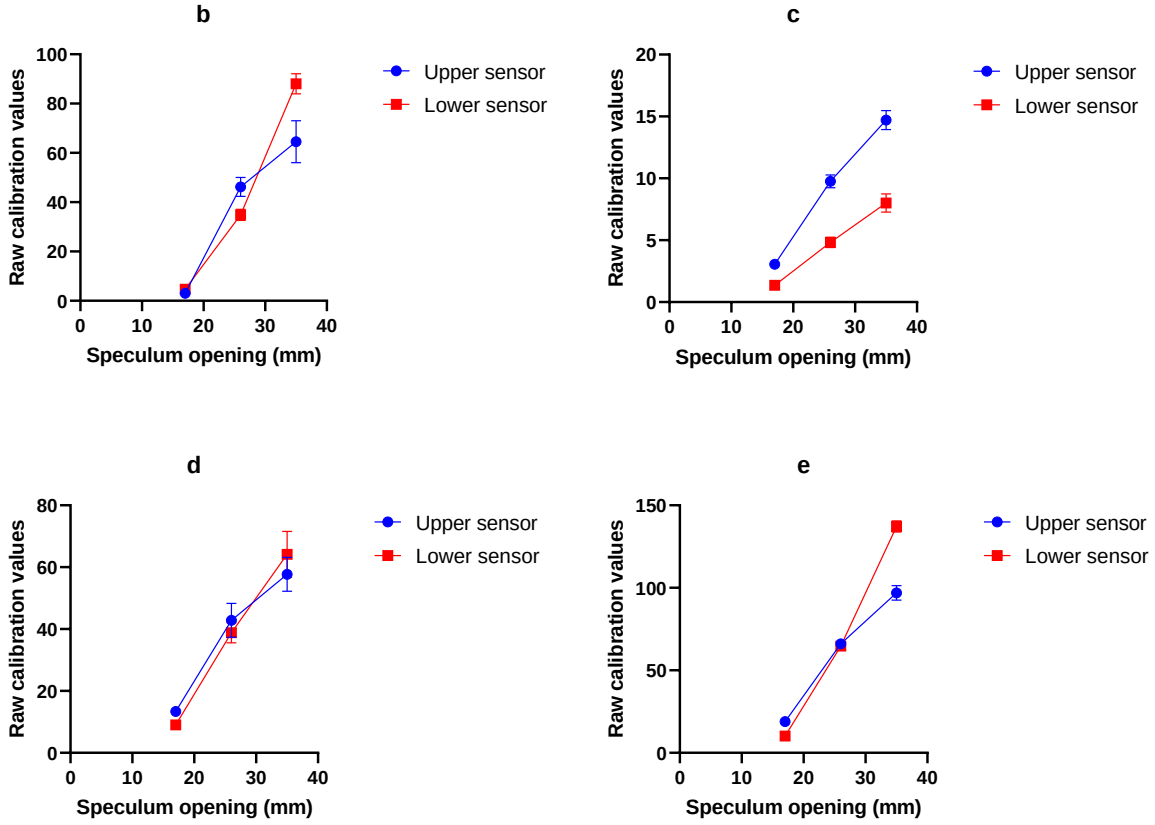

Figure 23: Mean raw values ± SEM (vertical axis) obtained in each form of power-law fit calibration (b, c, d and e) for each calibration point (horizontal axis)

Although calibration protocol *b* was more adequate for this application than protocol *a*, the results were inconsistent as the calibration points were too low. This did not present a problem for later trials as this type of calibration was only used with latex samples as the force ranges were too low for *ex vivo* testing. Using low sensitivity sensors in calibration *c* resulted in a smaller range of raw calibration values which introduced many errors as the highest speculum opening produced a lower raw value for the lower sensor than the upper sensor in intermediate dilation.
In calibration *d*, the high force range introduced by the potentiometer adjustment resulted in inconsistent raw values, which would not be reliable for testing. A balance between sensor type and potentiometer adjustment was found in calibration *e*, which allowed for more consistent calibration cycles and an appropriate force range.

5.2 Glove finger testing results

Sensor readings are presented here in mean values because measurements were taken after the sensors stabilized and plots generated were mostly horizontal, and unchanged. The exception to this was a few errors and fluctuations due to unpredictable external factors (for example, instability of the work surface), but those results were discarded and replaced with new tests as they were not relevant to this work.

Because the tape necessary to attach the sensors to the speculum had not yet been obtained until test 4 of the nitrile samples, there is a noticeable variation in force distributions between upper

and lower sensors with each sample. It is very noticeable, for example, in tests performed on nitrile sample 11 at medium dilation, as shown in figure 24.

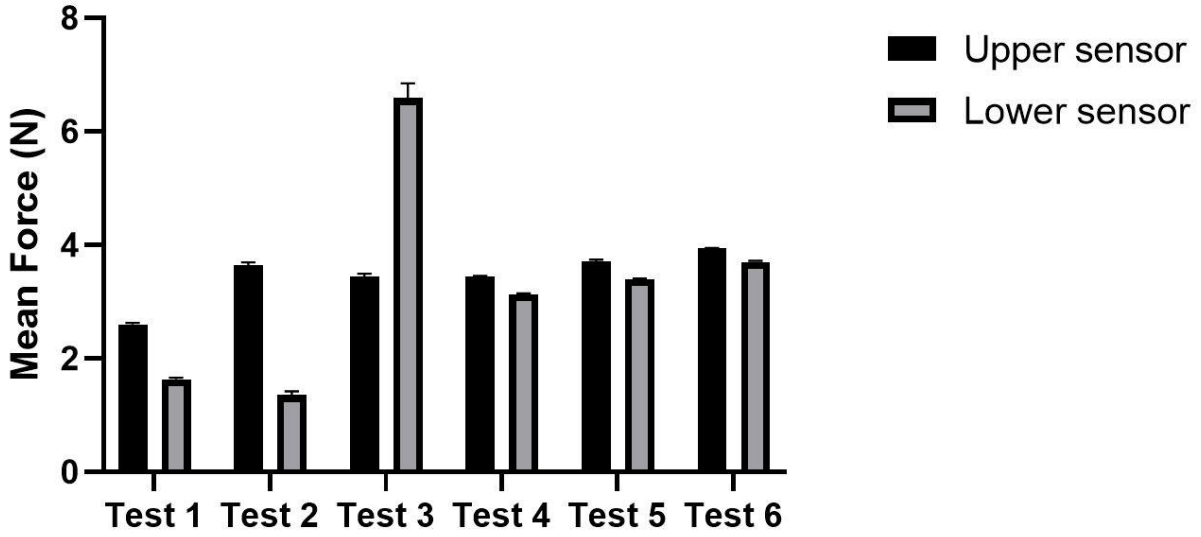

Figure 24: Mean force values ± SEM of upper and lower sensor readings for medium dilation (26 mm) for test 1 through 6 of nitrile sample 11

Mean values of the sensor readings and tensile test curves of latex samples at each dilation point are presented in Figures 25-28.

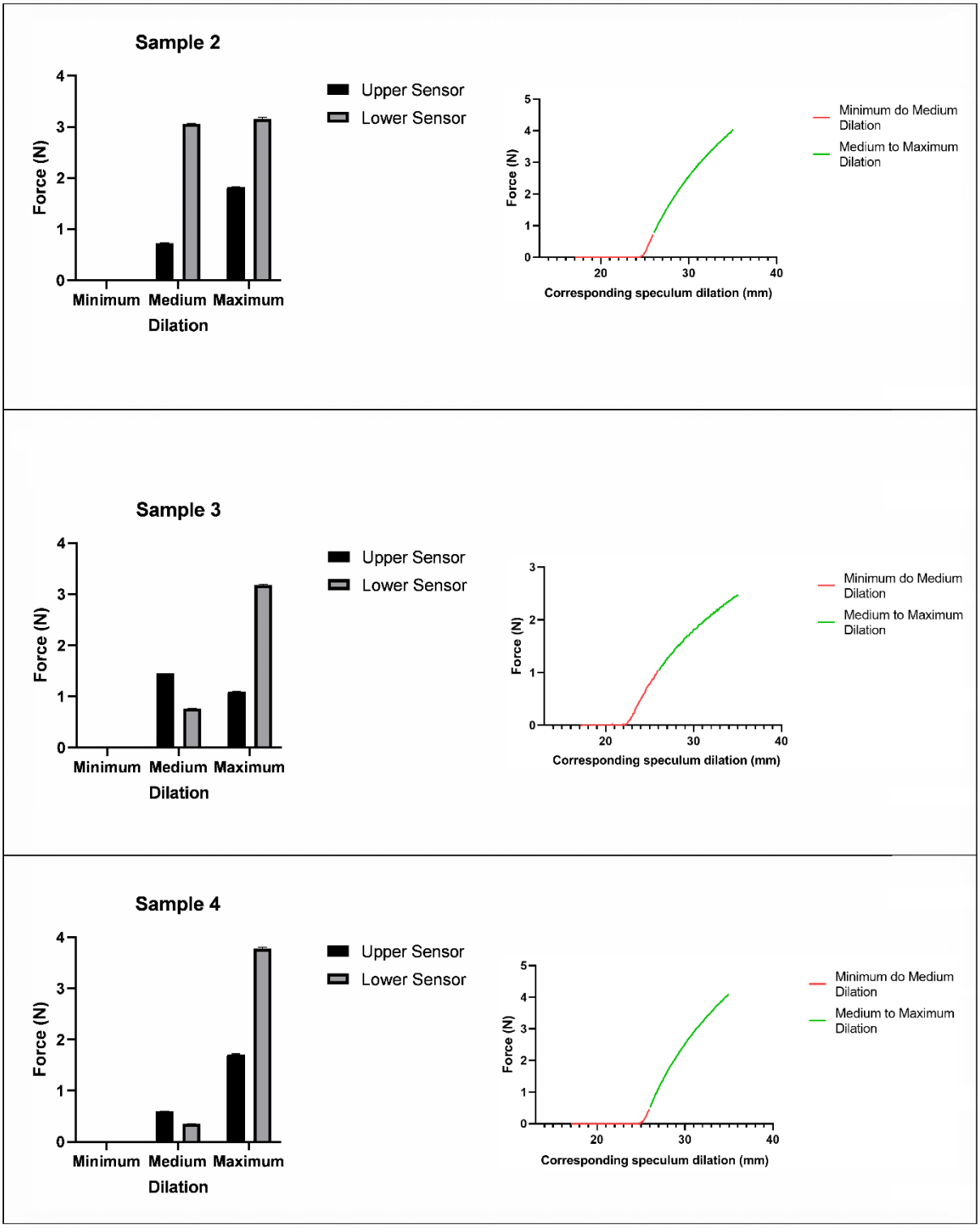

Figure 25: Left: mean force values ± SEM of upper and lower sensor readings for each dilation (minimum 17 mm, medium 26 mm, and maximum 35 mm) for n=2 measurements of latex samples 2, 3 and 4; Right: tensile test results in load-distance curves for the respective samples (from minimum opening of 17 mm to medium of 26 mm, medium to maximum of 35 mm)

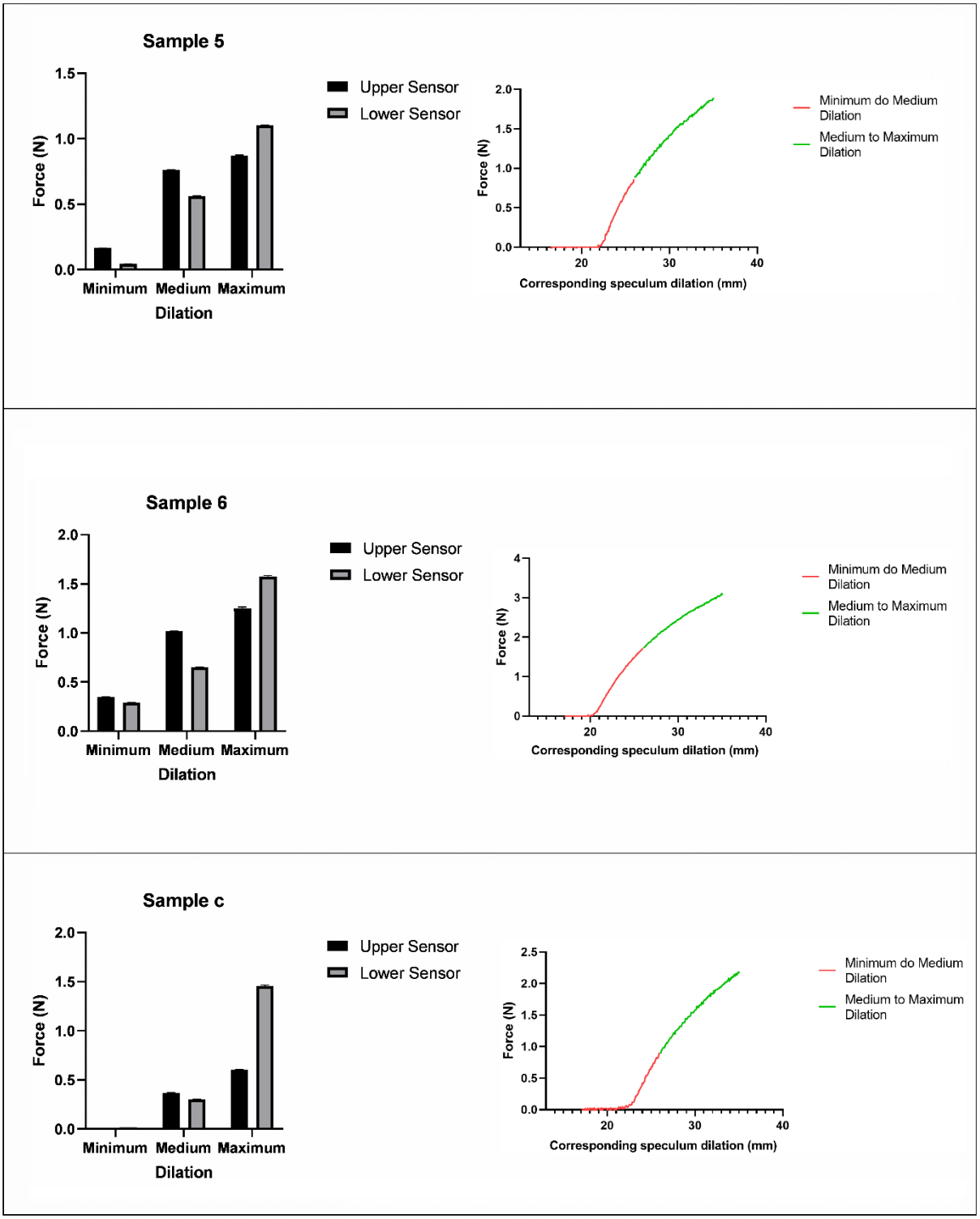

Figure 26: Left: mean force values ± SEM of upper and lower sensor readings for each dilation (minimum 17 mm, medium 26 mm, and maximum 35 mm) for n=2 measurements of latex samples 5, 6 and c; Right: tensile test results in load-distance curves for the respective samples (from minimum opening of 17 mm to medium of 26 mm, medium to maximum of 35 mm)

Latex tests, as previously mentioned, were performed with sensors adjusted and calibrated for low force ranges, and some results were inconsistent with tensile test results.

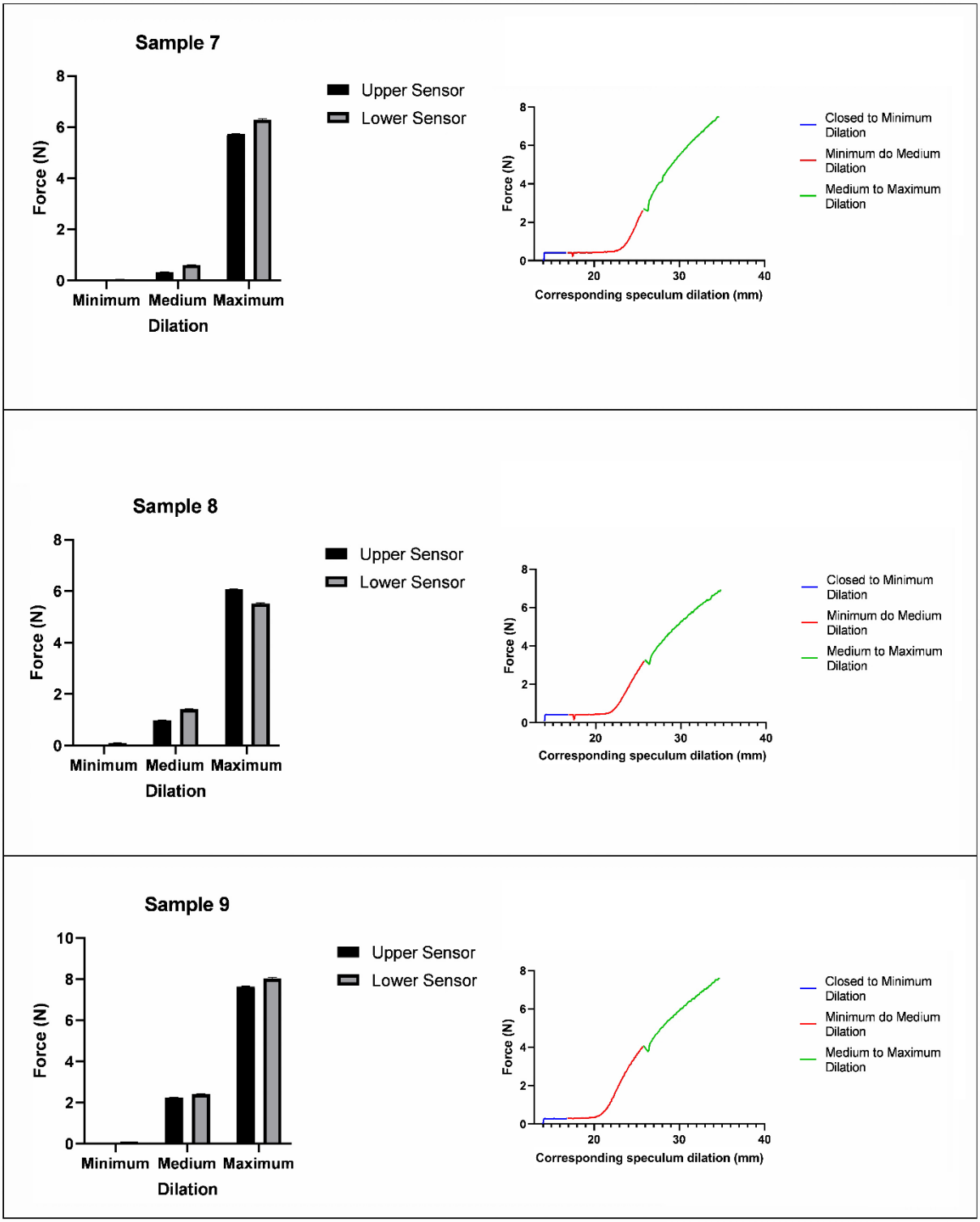

Figure 27: Left: mean force values ± SEM of upper and lower sensor readings for each dilation (minimum 17 mm, medium 26 mm, and maximum 35 mm) for n=2 measurements of nitrile samples 7, 8 and 9; Right: tensile test results in load-distance curves for the respective samples (from closed test pieces to a minimum opening of 17 mm, from minimum to medium of 26 mm, medium to maximum of 35 mm)

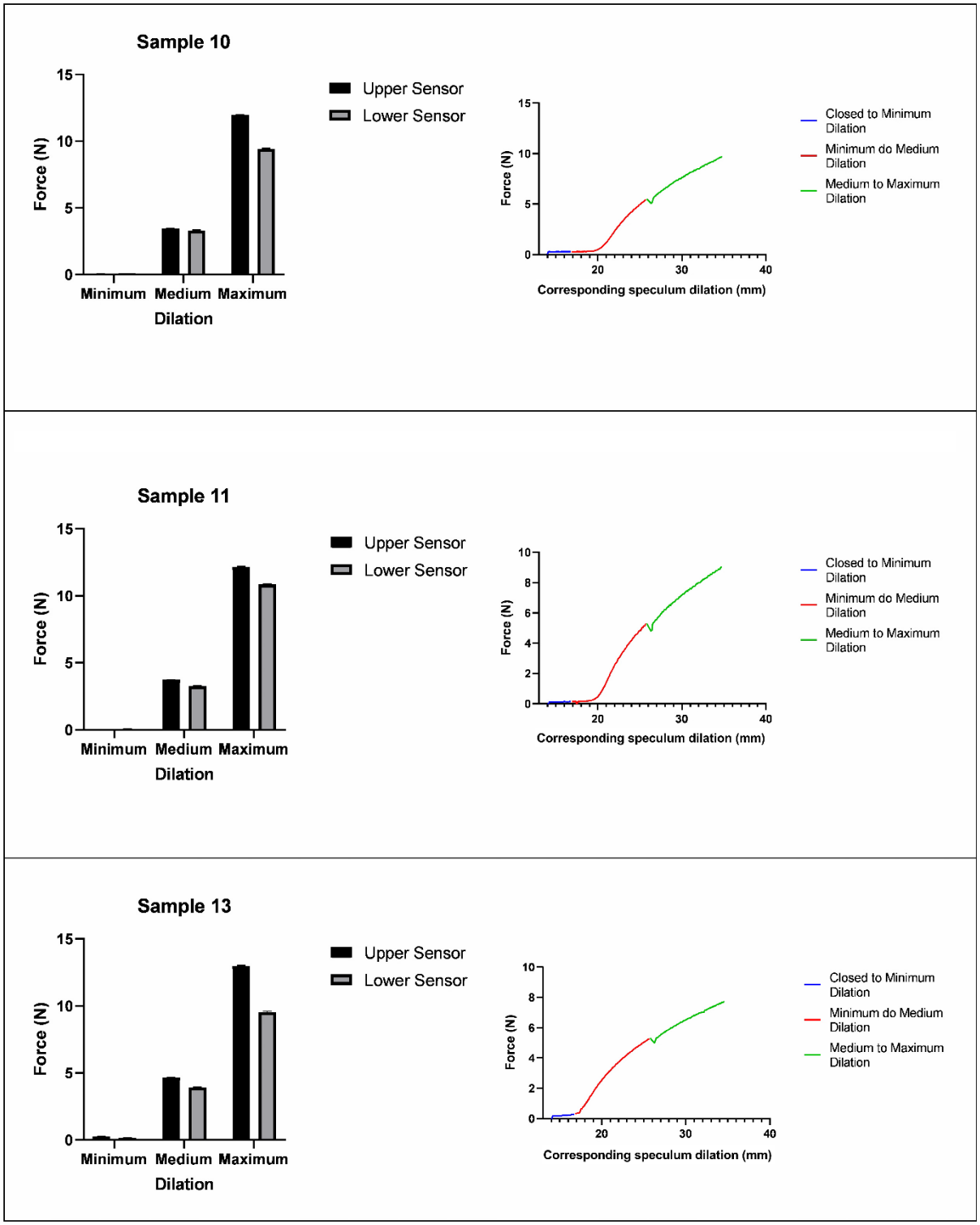

Figure 28: Left: mean force values ± SEM of upper and lower sensor readings for each dilation (minimum 17 mm, medium 26 mm, and maximum 35 mm) for n=2 measurements of nitrile samples 10, 11 and 13; Right: tensile test results in load-distance curves for the respective samples (from closed test pieces to a minimum opening of 17 mm, from minimum to medium of 26 mm, medium to maximum of 35 mm)

In lower dilations, samples with higher cross-section diameter (7 and 8) generated higher force values in the tensile tests, and this influence was not present in speculum readings. The decreased cross-section diameter from sample 7 and samples 9 to 13 resulted in higher force readings. However, the speculum sensors (particularly the upper sensor) presented higher force readings of samples with decreased diameters than tensile tests.

As shown in figure 29, nitrile specimen test results followed a mostly linear distribution upon eliminating minimum dilation readings, with a 0,2710 slope and a standard error of 0,03016. Latex specimen tests (figure 30) resulted in a primarily linear tendency, albeit with significant errors.

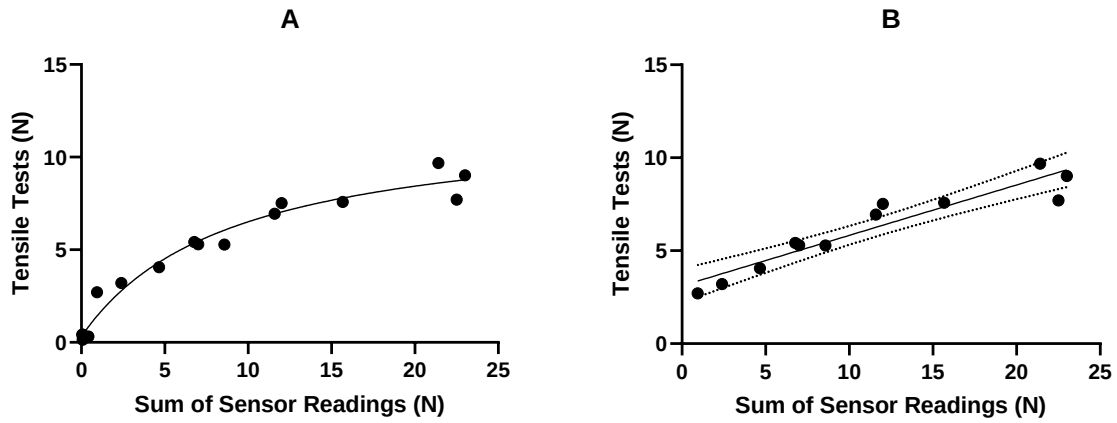

Figure 29: Scatter plots of average nitrile specimen sums of both sensor readings vs. tensile test results with nonlinear fit and simple linear regression (confidence level of 95%); (A) all tests; (B) excluding minimum dilation

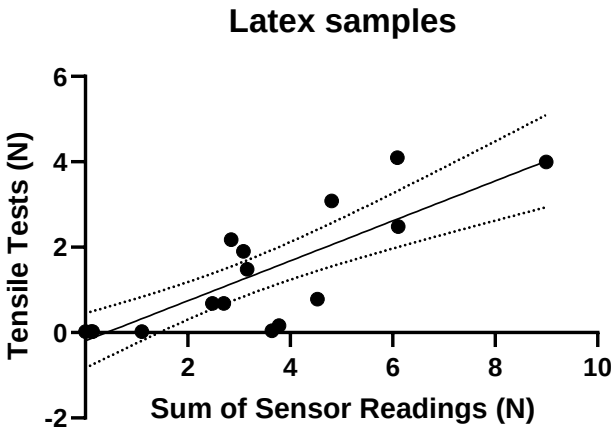

Figure 30: Scatter plot of average latex specimen sums of both sensor readings vs. tensile test results with simple linear regression (confidence level of 95%)

5.3 *Ex vivo* testing results

Results presented in figures 31 through 33 are upper and lower sensor readings of the vaginal specimen tested with speculum and the tensile test results of the vaginal specimen between consecutive dilations. Whenever possible, tensile tests went slightly beyond the maximum dilation reached in the speculum tests to showcase tissue relaxation upon reaching said opening (figure 31, sample 1-2; figure 32, samples 2-2 and 2-3; figure 33, sample 3-1 and 3-3). Difficulty in timing the recording of data and adjustment of the speculum dilation and the sample resulted in some plots showing the movement of opening the device (figure 33, samples 3-1 and 3-3), and others were mainly showing stabilized readings (figure 31, sample 1-2 at medium opening). For this analysis only the stabilized portions of the plots were considered, and the tensile test results around the respective dilation both represent the readings upon relaxation of the tissues. The distribution of forces between sensors depends on the placement of the sample on the speculum and, in some cases (figure 32, sample 2-1 at 28.2 mm opening, and sample 2-2 at minimum opening), force values have changed during the measurements as had happened in some glove finger tests.

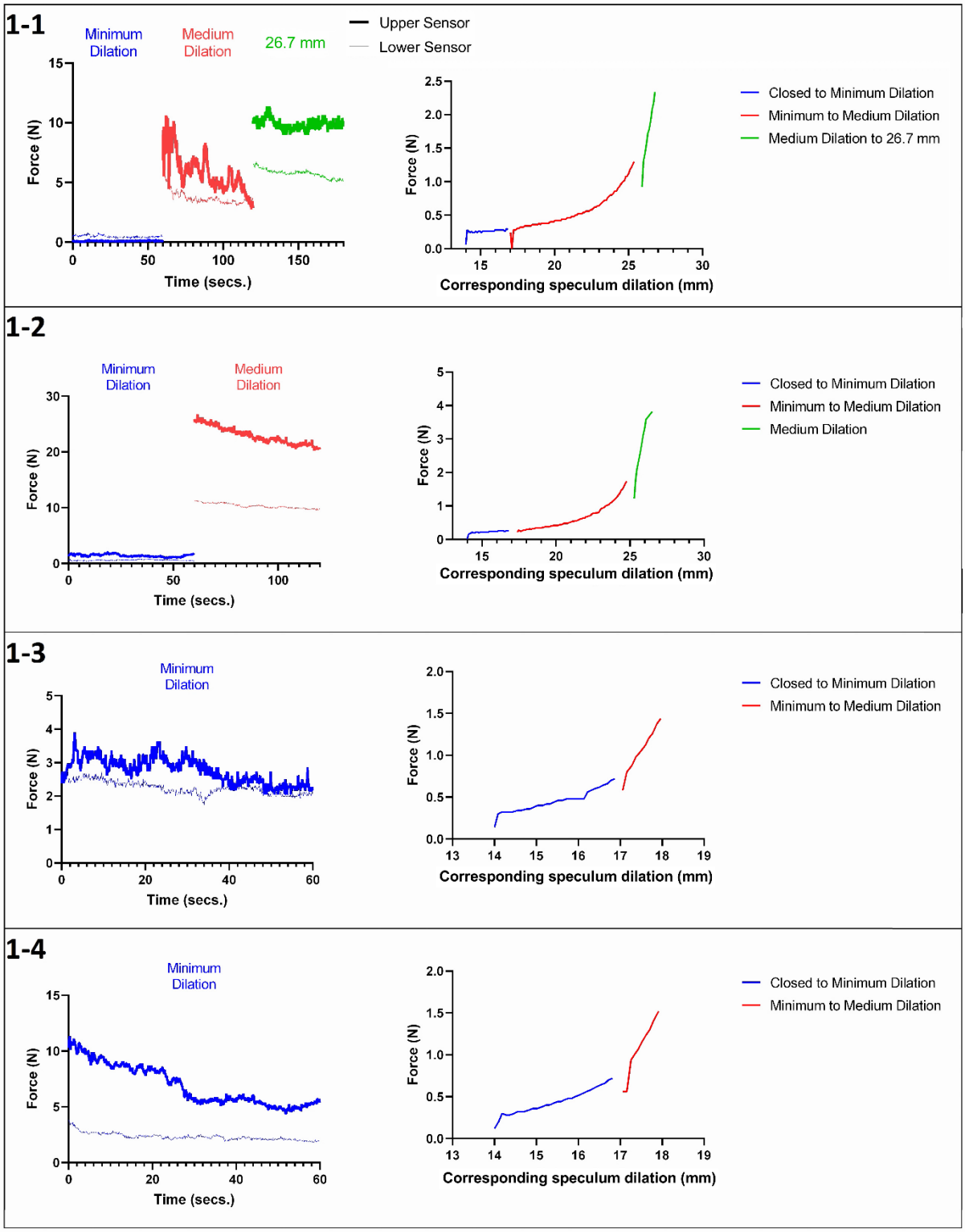

Figure 31: Speculum test load-time plots (left) and tensile test load-distance curves (right) of specimen 1 (samples 1-1 through 1-4) for each dilation used (minimum of 17 mm, medium 26 mm, and maximum 35 mm or otherwise specified)

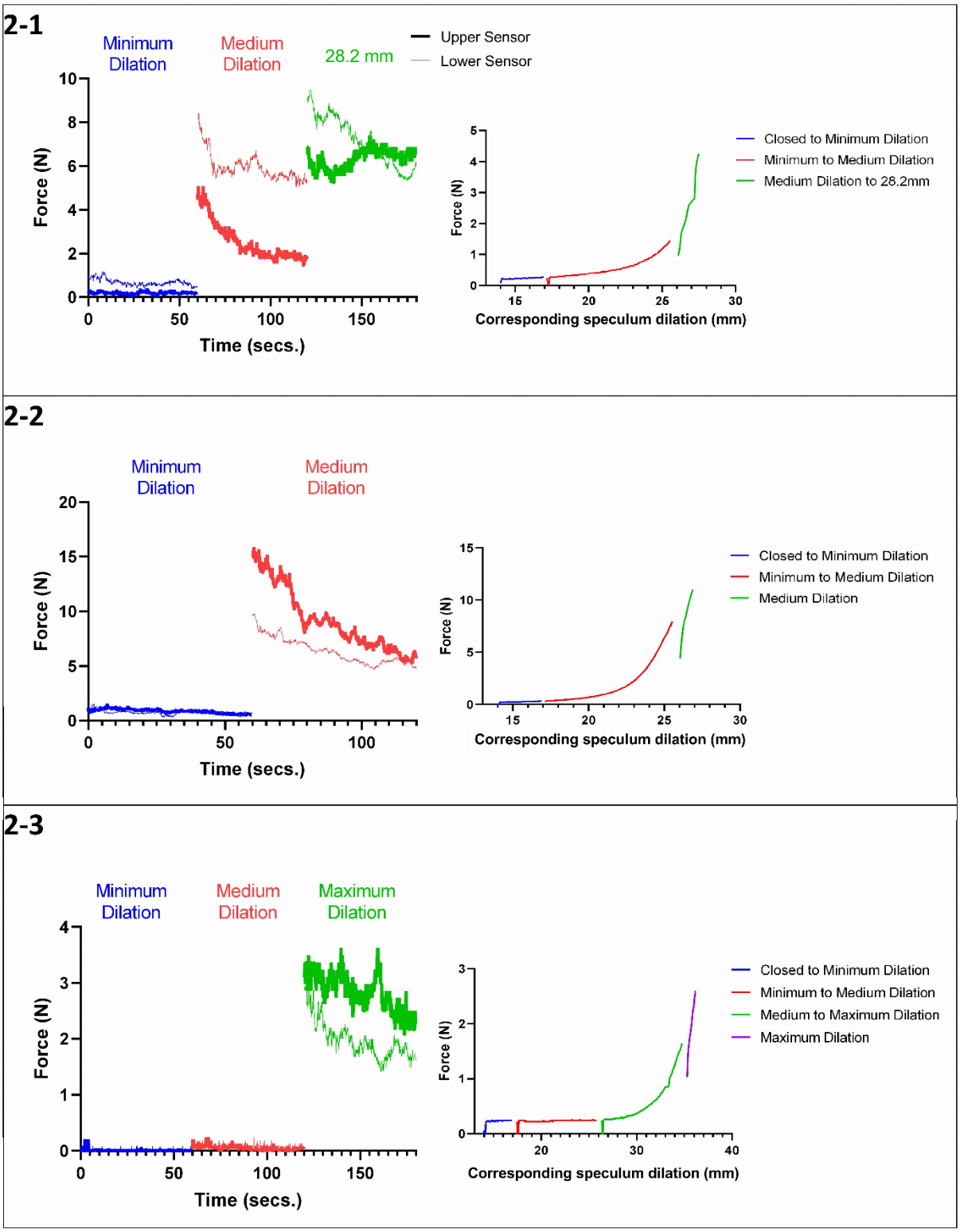

Figure 32: Speculum test load-time plots (left) and tensile test load-distance curves (right) of specimen of specimen 2 (samples 2-1 through 2-3) for each dilation used (minimum of 17 mm, medium 26 mm, and maximum 35 mm or otherwise specified)

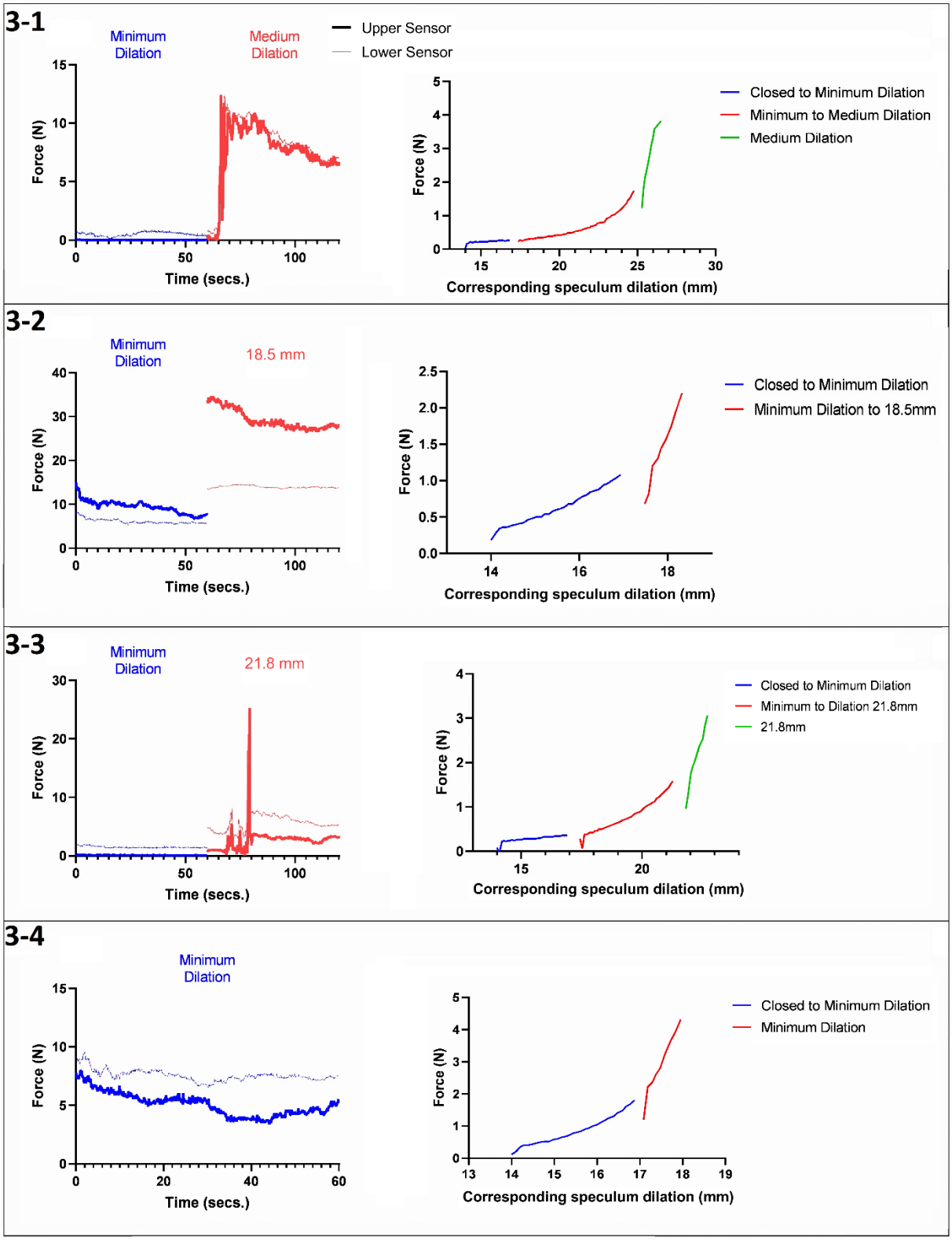

Figure 33: Speculum test load-time plots (left) and tensile test load-distance curves (right) of specimen 3 (samples 3-1 through 3-4), for each dilation used (minimum of 17 mm, medium 26 mm, and maximum 35 mm or otherwise specified)

Between tensile and speculum test results at the minimum dilation, a higher ratio was obtained in samples 1-1, 2-1 and 3-1, which were part of the distal vagina, and thus contained tissue from the urethra, increasing their cross-section.

Most of the samples were more rigid than anticipated upon calibration, and as such, sensor measurements above 10 N may not be accurate, as was the case of samples 1-2 and 3-2. This increased rigidity required changes to dilations on both tests for some of the samples. As predicted, relaxation of the tissues during speculum testing resulted in lower readings in the subsequent tensile test, and in the cases of some of the more rigid samples (1-2, 3-1, 3-2) this difference increased.

The upper sensor did not respond as expected during the sample 3-3 testing at minimum dilation, which had previously happened with some glove samples. However, to avoid unnecessary changes to the sample, the test was not repeated.

Sample 2-3 produced results inconsistent with the other samples due to its greater looseness. At low and medium dilations, the force readings were remarkably higher in the tensile test than in the device since the sample rests on the body of the speculum, and only a fraction of its weight is supported by the upper sensor. Sample 2-2 seems to produce results between those obtained from 2-1 and 2-3.

Within the same vaginal samples (1 and 3), it was found that specimens produced higher force readings the closer they were to the cervix; the opposite was verified for vaginal sample 2.

Upon elimination of test results that presented significant errors, previously explained, it was found (as showcased in table 2) that the mean ratio between tensile test results and the sum of sensor results was of 0,1425 with a standard error of 0,02576 owed to errors associated with sample placement, differences in sample inner diameters, displacement of tensile test pieces, and system noise. Based on the elimination of errors, the test results distribution was mainly linear, as shown in figure 34, previously explained.

Table 2: Average stabilized readings of upper and lower sensors and tensile test values around the corresponding dilation and their ratio

Sample	Dilation (mm)	Upper sensor (N)	Lower sensor (N)	Tensile test (N)	Ratio
1-2	17	1,45326	0,74508	0,254	0,1155
1-3	17	2,34115	2,12956	0,752	0,1682
1-4	17	5,29797	1,49892	0,716	0,1053
3-4	17	4,21186	0,60729	0,263	0,3278
1-1	26	5,61303	0,61969	0,319	0,2634

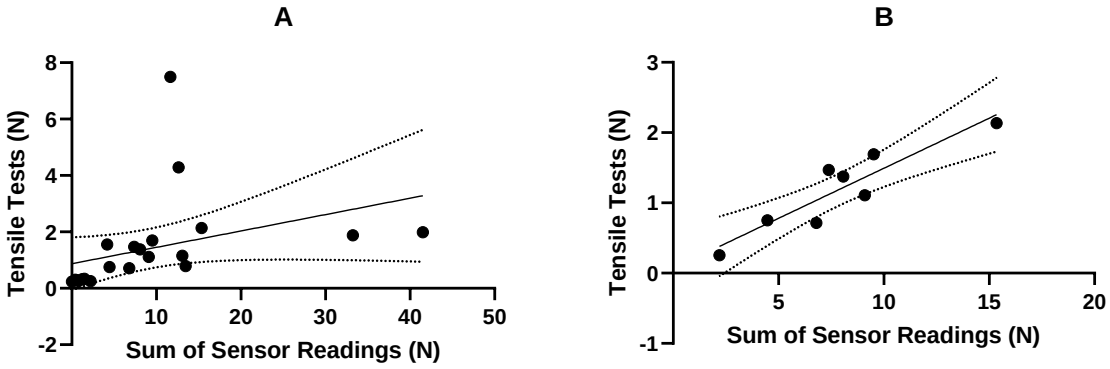

Figure 34: Scatter plots of average relaxed tissue sums of both sensor readings vs. tensile test results with simple linear regression (confidence level of 95%); (A) all tests; (B) excluding major errors

5.4 Discussion

The device was successfully used to discern variations in compliance of materials with different properties, dimensions, and speculum dilations. It was found to be responsive to differences in cross-section diameter and rigidity, which is advantageous for detecting changes associated with POP development.

A common problem among previously analyzed devices is that they require many sensors, fragile components, temperature dependency, or expensive equipment to measure pelvic floor characteristics (Egorov, Raalte and Sarvazyan 2010) (van Raalte and Egorov 2015) (Parkinson, Gargett, et al. 2016) (Parkinson, Rosamilia, et al. 2019) (Guaderrama, et al. 2005). This project's device could discern with only two sensors and through varying fixed dilations. Although with the current device prototype, only a small portion of the anterior and posterior vaginal walls can be analyzed. Replacing these sensors with pressure mapping sensors would allow for measurements of pressure distributions over a greater length of the vagina whilst using the same fixed dilations method. The use of a standard speculum also proved to be easy to use with *ex vivo* vaginal samples, thanks to its shape already being adapted for gynaecology applications, though less so with the glove samples due to increased friction. The combination of thin sensors and the female condoms makes the device minimally invasive and likely to be able to adapt to varying anatomies of different patients, making the diagnostic process more comfortable for the patient than using other probe devices (Egorov, Raalte and Sarvazyan 2010) (van Raalte and Egorov 2015).

The Excel MicroView reader, used in this work, allowed for a simple, visual result representation and quick, intuitive interpretation and comparison. The high amount of noise previously mentioned created unnecessary distractions, and it would have been more practical to round these values to a more realistic number of significant figures.

Calibration

The accuracy of measurements was heavily dependent on the calibration protocol used. Using low force points, limited the force range, the sensor could accurately measure while using calibration points with larger forces made smaller readings inaccurate. The latter occurred with glove tests, where the lowest dilation results were entirely inconsistent. It is, however, also owed to the limited sensitivity to these low readings of the tensile test machine.

The same limitation in low dilation readings was also found when using sensors of lower sensitivity, and these could not accurately measure the smaller loads used in this work no matter which potentiometer adjustment was used and was thus not useful in this application.

Calibrated sensor outputs presented a very high number of significant figures regardless of the calibration method. These did not result from a the resolution but likely from the equations used for calibration, and the result was a high amount of noise, primarily noticeable in tests with smaller loads.

The linear-fit method resulted in higher repeatability of calibration raw readings due to the ease of performing a consistent calibration protocol when resting the sensors on a flat surface and placing weights in the centre of the sensing area. However, this method is not indicated for reading load distributions in compliant materials, and it requires constant disassembly and reassembly of the device to place the sensors on a flat surface and the speculum.

Calibration methods used introduce inconsistencies with variations in sample cross-section since calibration values were obtained from a tensile test. As such, a more reliable way of applying known loads could be a sleeve shaped inflatable bladder around the speculum.

It was found that tests performed before the necessary material to fixate the sensors to the speculum blades were acquired resulted in inconsistent results. It was very evident in latex specimen tests and the first nitrile specimen tests. A consistent fixation of sensors is critical to ensure they always rest on the exact location of the speculum blades, as readings are heavily dependent on the shape of the surface they're pressed against. This dependency on surface shape was demonstrated by the differences in raw calibration values obtained between upper and lower sensor in power-law fit calibrations. It will be equally crucial for clinical tests to guarantee that the same region of the vaginal wall is measured across tests. The use of female condoms as device protection did not result in visible interference in the readings.

Glove and vaginal tissue testing

Sensor calibration for the tissue testing was made for force ranges found in clinical trials by Amorim, *et al.* (2017), which was not large enough for some of the *ex vivo* vaginal samples used in this work. This is likely due to a combination of differences in anatomy, as previously mentioned, and tissue degradation post mortem and the shortening of the smooth muscle from *rigor mortis* leading to the stiffening of the tissues. This loss of elasticity corresponds to lower compliance of the materials and higher force readings (Rattenbury 2018).

Higher device response to differences in sample surface areas was observed in glove finger tests than in *ex vivo* vaginal tissue tests, likely due to the lack of lubrication in tests using these samples. The speculum blades have a larger surface area in contact with the samples than the designed and printed blades used for tensile tests. Latex and nitrile gloves were designed to avoid slip and thus had much friction with the surface of the speculum, whilst in *ex vivo* vaginal tissues tests, the tissue was wet and the condoms used were lubricated and allowed the tissue to stretch freely around the speculum blades. Different glove materials also resulted in different frictions, adding more variation to the results. However, in all cases, there was an increased response to higher dilations, the results of which, excluding errors, were proportional to tensile test results.

As previously mentioned, there is a correlation between POP and a decrease in the smooth muscle of the vaginal wall and collagen content and quality. The use of excised vagina samples in this work allowed for collecting data on the individual vaginal wall properties, and the differences between each vaginal specimen were very noticeable. The device detected apparent differences in vaginal wall behaviour in different sections, but it is not known if the exact placement of these variations is consistent with human anatomy. Despite having similar ligament insertions to humans, the pig is a prostrate quadruped with a different pelvic orientation. Thus, the mechanisms of prolapse are expected to be different, with the organs collapsing in different directions, possibly resulting in different changes in properties of the smooth muscles of the vaginal wall (Kerkhof, Hendriks and Brölmann 2009) (Couri, et al. 2012).

Many errors were encountered due to limitations in the experimental procedure, but these were unavoidable to compare tensile test results. By dividing each vagina into specimens, the properties of the original organism were altered, and factors such as the force of gravity, tissue relaxation and differences in cross-section area interfered with the results. However, it was possible to perform tensile tests for comparison, which would be impossible using the entire vagina length of the vagina was used, and the results of the readings were otherwise consistent.

Ex vivo vaginal sample 2-3 produced results inconsistent with the other samples because it was rather loose. Force readings were attributed to the weight of the sample rather than the compliance of tissues. The sample rested on the upper blade of the speculum, and only a small area was in contact with the upper sensor, whilst in the tensile test, the entire weight was recorded by the load cell. It resulted in much higher force readings during the tensile test than

the device. These readings would have likely been more accurate if taken *in vivo* as the sample would not be hanging from the speculum. Despite these limitations, it was possible to obtain more accurate results in sample 2-3 during the highest dilation, as the speculum blades had complete contact with the tissues. However, with tensile tests inconsistencies and limitations in the testing protocol, the device could discern a significant loss of firmness in tissues in this sample. Samples 2-2 and 2-1 had higher load readings than 2-3, with 2-2 being slightly higher. It is consistent with readings obtained by Parkinson, *et al.* (2016) during *in vivo* studies on parous sheep, where sensors closest to the cervix registered lower loads, which then increased closer to the distal vagina and slightly decreased towards the vulva.

During the vaginal tissue testing, tensile test results corresponded to 0,1425 times the combined readings of upper and lower device sensors. That number is 0,271 for nitrile glove sample tests and 0,4678 for latex glove sample tests. Due to differences in material characteristics, the thickness of samples, and the relaxation of *ex vivo* vaginal samples resulting in lower comparable tensile test results. Likewise, it was observed that in tissue samples with a large cross-section area, near the vulva, this ratio was higher, going up to 0,73 (sample 3-1).

Although this device cannot diagnose enterocele and uterine prolapse as it does not take measurements of the proximal wall, it overcomes the limitation Guaderrama *et al.* (2005) of erroneously measuring atmospheric pressure. Using the dilation of the speculum blades to press the sensors against the surface of the vaginal walls, contact with air is eliminated. It would only present a problem when using the smallest dilation on a specimen with a significantly reduced elastic modulus as was the case of sample 2-3 (assuming this degree of firmness reduction could occur in the distal vagina, whereas sample 2-3 was taken from the proximal vagina), but this is solved when using other dilations, thus demonstrating the versatility of the device.

The sampling rate was sufficient to resolve the slow changes in load associated with tissue relaxation and sudden changes introduced by speculum dilation. This rate will allow the diagnosis of incontinence in clinical trials as it can discern changes in load distribution during a prolonged contraction.

6 Conclusions and future works

This work contributed to the intravaginal pressure (IVP) measurement device development, demonstrating the viability of the concept of using a speculum with parallel blades, varying dilation to measure the contact force, associated with the compliance of vaginal walls; determining the best method of performing calibration and tests, and, through assembly, adjustments and experimentation, comprehending the requirements and further alterations necessary for future works.

It was shown to be able to perform the same measurements as other similar devices with less complex and more affordable equipment, though clinical trials will be necessary to assess and compare other aspects not covered by this work's methods.

The sensitivity and resolution of the sensors used in this work allowed to obtain the desired results with the proper calibration. For this work, using two contact force sensors to measure materials' compliance was a cheap and practical solution that produced the intended results. For later stages of development, pressure mapping sensors are to be used instead to provide a complete pressure profile throughout the length of the vaginal wall and detect spatial variations. The sampling rate used was sufficient for passive testing, but clinical studies will be necessary to determine if a higher rate will be needed to discern more dynamic events like coughing.

Due to the choice of procedure carried out in this work, it was impossible to discern differences between the anterior and posterior vaginal wall measurements, which would be interesting to investigate in future works.

The varying dilations of the speculum allowed to identify differences in material properties of various samples without the need for voluntary contractions. Factors such as tissue firmness, sample diameter and cross-section all influenced the results measured by the speculum sometimes differently from how they influenced tensile test results.

The device must be modified to have a sleeker design with communication with software through Bluetooth, making it more practical for clinical use. It must also have fixed dilation markers.

Future works

Future *in vivo* and clinical trials will allow to test how this device performs when the effects of IAP are present, how it detects the characteristics of surrounding pelvic floor tissue, and how the dilation of the speculum compares to coughing and Valsalva manoeuvre. Future clinical tests will also determine how well patients tolerate this type of diagnosis. Anatomic characteristics of this work's test subjects and the stiffening effect of post-mortem processes limited the range of dilation of the speculum. It is expected that some patients (particularly nulliparous) will also be unable to tolerate some speculum dilations, but this shouldn't pose a problem as diagnosis with this device is to include the active performance of contractions and Valsalva.

In the next stage of development, this device will be used in *in vivo* experimental trials of unconscious ovine subjects. It will be possible to collect data on the pressure profiles of the anterior and posterior vaginal walls along a greater length of the vagina using pressure mapping sensors and the influence of pelvic floor muscles and IAP (simulated by placing varying loads over the sheep's abdomen). Biopsies will be taken to compare device measurements with tissue elasticity obtained in a wider variety of tests.

Clinical trials will constitute the following development stage, where comfort to the patients during diagnosis will be tested to make any possible adjustments to the procedure. Data will be collected on diagnosis with different strains (passive, coughing, Valsalva, contraction) and the

influence of IAP and surrounding pelvic floor tissue. Patients may be instructed to perform a contraction over some time to evaluate variation in the strength of contraction to diagnose urinary incontinence. With enough test subjects, it will be possible to collect data for machine learning algorithms used for automatic diagnosis, not requiring physicians to be knowledgeable in exact pressure measurements of the pelvic floor. It will also provide information on vaginal properties to be used in computational models to simulate the behaviour of the pelvic floor.
This work is intended to be published in an article for a scientific journal.

7 References

©Tekscan Inc. 2018. "Tekscan." 21 February. Accessed 2018. https://www.tekscan.com/products-solutions/electronics/flexiforce-prototyping-kit.

—. 2021. "Tekscan." Accessed March 2021. https://www.tekscan.com/products-solutions/force-sensors/a201.

Alas, A. N., and J. T. Anger. 2015. "Management of apical pelvic organ prolapse." *Current urology reports* 16 (5): 33.

Amorim, A. C., L. P. Cacciari, A. C. Passaro, S. R. Silveira, C. F. Amorim, J. F. Loss, and I. C. Sacco. 2017. "Effect of combined actions of hip adduction/abduction on the force generation and maintenance of pelvic floor muscles in healthy women." *Plos one* 12 (5).

Ashton-Miller, James A., and J. O. DeLancey. 2014. "Functional anatomy of the female pelvic floor." In *Evidence-Based Physical Therapy for the Pelvic Floor*, 19-33. Churchill Livingstone.

BASYS Beratungsgesellschaft für angewandte Systemforschung mbH, WifOR, Gesundheitsökonomisches Zentrum der TU Dresden (GÖZ), TU Berlin, IEGUS. 2015. *National Health Account for Germany.* Berlin: The Federal Ministry for Economic Affairs and Energy.

Bhadana, P. 2020. "Pelvic Organ Prolapse: Examination and Assessment." In *Lower Urinary Tract Dysfunction: From Evidence to Clinical Practice*, 11-23. IntechOpen.

Blaivas, J. G., R. S. Purohit, M. S. Benedon, G. Mekel, M. Stern, M. Billah, and V. Iakovlev. 2015. "Safety considerations for synthetic sling surgery." *Nature Reviews Urology* 12 (9): 481–509.

Bø, K. 2012. "Pelvic floor muscle training in treatment of female stress urinary incontinence, pelvic organ prolapse and sexual dysfunction." *World Journal of Urology* 30 (4): 437–443.

Brunner, L. S., S. C. O. Smeltzer, and D. S. Suddarth. 2010. *Brunner & Suddarth's textbook of medical-surgical nursing.*

Bump, R. C., A. Mattiasson, K. Bø, L. P. Brubaker, J. O.L. DeLancey, P. Klarskov, B. L. Shull, and A. R.B. Smith. 1996. "The standardization of terminology of female pelvic organ prolapse and pelvic floor dysfunction." *American journal of obstetrics and gynecology* 175 (1): 10-17.

Cacciari, L. P., and I. C. Sacco. 2019. "Pelvic floor biomechanical assessment: current approaches and new evidence." In *DHM and Posturography*, 321-330. Academic Press.

Clark, T. D. 2007. *PharmaHandbook: A Guide to the International Pharmaceutical Industry.* New Orleans: Value of Insight Consulting, Inc.

Couri, B. M., A. T. Lenis, A. Borazjani, M. F. R. Paraiso, and M. S. Damaser. 2012. "Animal models of female pelvic organ prolapse: lessons learned." *Expert review of obstetrics & gynecology* 7 (3): 249-260.

Daneshgari, F., W. Kong, and M. Swartz. 2008. "FDA Public Health Notification: serious complications associated with transvaginal placement of surgical mesh in repair of pelvic organ prolapse and stress urinary incontinence." *European urology* (Food and Drug Administration, Silver Spring, Md, USA) 55 (5): 1235-1236.

DeLancey, J. O. L. 2016. "Pelvic floor anatomy and pathology." In *Biomechanics of the female pelvic floor.*, 13-51. Academic Press.

Department of Health. 2009-10. *Department of Health: Resource Accounts.* London: UK by The Stationery Office.

Egorov, V., H. van Raalte, and A. P. Sarvazyan. 2010. "Vaginal tactile imaging." *IEEE Transactions on Biomedical Engineering* 57 (7): 1736-1744.

Epstein, L. B., C. A. Graham, and M. H. Heit. 2007. "Systemic and vaginal biomechanical properties of women with normal vaginal support and pelvic organ prolapse." *American journal of obstetrics and gynecology* 167 (2): 165-e1.

Ghetti, C., W. T. Gregory, S. R. Edwards, L. N. Otto, and A. L. Clark. 2005. "Severity of pelvic organ prolapse associated with measurements of pelvic floor function." *International Urogynecology Journal* 16 (6): 432-436.

Guaderrama, N. M., C. W. Nager, J. Liu, D. H. Pretorius, and R. K. Mittal. 2005. "The vaginal pressure profile." *Neurourology and Urodynamics: Official Journal of the International Continence Society* 24 (3): 243-247.

Handa, V. L., E. Garrett, S. Hendrix, E. Gold, and J. Robbins. 2004. "Progression and remission of pelvic organ prolapse: a longitudinal study of menopausal women." *American journal of obstetrics and gynecology* 190 (1): 27-32.

Haylen, B. T., et al. 2010. "An International Urogynecological Association (IUGA)/International Continence Society (ICS) joint report on the terminology for female pelvic floor dysfunction." *Neurourology and Urodynamics: Official Journal of the International Continence Society* 29 (1): 4-20.

Hendrix, S. L., A. Clark, I. Nygaard, A. Aragaki, V. Barnabei, and A. McTiernan. 2002. "Pelvic organ prolapse in the Women's Health Initiative: gravity and gravidity." *American journal of obstetrics and gynecology* 186 (6): 1160-1166.

Jelovsek, J. E., and M. D. Barber. 2006. "Women seeking treatment for advanced pelvic organ prolapse have decreased body image and quality of life." *American journal of obstetrics and gynecology* 194 (5): 1455-1461.

Jelovsek, J. E., C. Maher, and M. D. Barber. 2007. "Pelvic organ prolapse." *The Lancet* 369 (9566): 1027-1038.

Jundt, K., U. Peschers, and H. Kentenich. 2015. "The investigation and treatment of female pelvic floor dysfunction." *Deutsches Ärzteblatt International* 33-34.

Kenton, K., and E. R. Mueller. 2006. "The global burden of female pelvic floor disorders." *BJU international* (98): 1-5.

Kerkhof, M. H., L. Hendriks, and H. A. M. Brölmann. 2009. "Changes in connective tissue in patients with pelvic organ prolapse—a review of the current literature." *International Urogynecology Journal* 461-474.

Lamers, B. H., B. M. Broekman, and A. L. Milani. 2011. "Pessary treatment for pelvic organ prolapse and health-related quality of life: a review." *International urogynecology journal* 22 (6): 637-644.

Lazarou, G., E. Minis, and B. Grigorescu. 2019. "Outcomes of stress urinary incontinence in women undergoing TOT versus Burch colposuspension with abdominal sacrocolpopexy." *International Urogynecology Journal.* 30 (2): 245-250.

Mascarenhas, T., M. Mascarenhas-Saraiva, A. Ricon-Ferraz, P. Nogueira, F. Lopes, and A. Freitas. 2015. "Pelvic organ prolapse surgical management in Portugal and FDA safety communication have an impact on vaginal mesh." *International urogynecology journal* 26 (1): 113-122.

Muscolino, J. E. 2014. *Manual therapy for the low back and pelvis: a clinical orthopedic approach.* Wolters Kluwer Health | Lippincott.

Olsen, A. L., V. J. Smith, J. O. Bergstrom, J. C. Colling, and A. L. Clark. 1997. "Epidemiology of surgically managed pelvic organ prolapse and urinary incontinence." *Obstetrics & Gynecology* 89 (4): 501-506.

Parkinson, Luke A., Anna Rosamilia, Shayanti Mukherjee, Anthony W. Papageorgiou, Joan Melendez-Munoz, Jerome A. Werkmeister, Caroline E. Gargett, and John W. Arkwright. 2019. "A fiber-optic sensor-based device for the measurement of vaginal integrity in women." *Neurourology and urodynamics* 38 (8): 2264-2272.

Parkinson, Luke A., Caroline E. Gargett, Natharnia Young, Anna Rosamilia, Aditya V. Vashi, Jerome A. Werkmeister, Anthony W. Papageorgiou, and John W. Arkwright. 2016. "Real-time measurement of the vaginal pressure profile using an optical-fiber-based instrumented speculum." *Journal of biomedical optics* 21 (12): 127008.

Rahn, D. D., M. D. Ruff, S. A. Brown, H. F. Tibbals, and R. A. Word. 2008. "Biomechanical properties of the vaginal wall: effect of pregnancy, elastic fiber deficiency, and pelvic organ prolapse." *American journal of obstetrics and gynecology* 198 (5): 590-e1.

Rattenbury, A. E. 2018. "Forensic taphonomy." In *Forensic Ecogenomics*, by T. Ralebitso-Senior, 37-59. Academic Press.

Rechberger, T., K. Postawski, J. A. Jakowicki, Z. Gunja-Smith, and J. F. Woessner Jr. 1998. "Role of fascial collagen in stress urinary incontinence." *Am J Obstet Gynecol* 179: 1511–1514.

Samuelsson, E. C., F. A. Victor, G. Tibblin, and K. F. Svärdsudd. 1999. "Signs of genital prolapse in a Swedish population of women 20 to 59 years of age and possible related factors." *American journal of obstetrics and gynecology* 180 (2): 299-305.

Schaffer, Joseph I., Clifford Y. Wai, and Muriel K. Boreham. 2005. "Etiology of pelvic organ prolapse." *Clinical obstetrics and gynecology* 48 (3): 639-647.

Schwertner-Tiepelmann, N., R. Thakar, A. H. Sultan, and R. Tunn. 2012. "Obstetric levator ani muscle injuries: current status." *Ultrasound in obstetrics & gynecology* 39 (4): 372-383.

Shaw, J. M., N. M. Hamad, T. J. Coleman, M. J. Egger, Y. Hsu, R. Hitchcock, and I. E. Nygaard. 2014. "Intra-abdominal pressures during activity in women using an intra-vaginal pressure transducer." *Journal of sports sciences* 32 (12): 1176-1185.

Stanford, E. J., A. Cassidenti, and M. D. Moen. 2012. "Traditional native tissue versus mesh-augmented pelvic organ prolapse repairs: providing an accurate interpretation of current literature." *International urogynecology journal* 23 (1): 19-28.

Subramanian, D., K. Szwarcensztein, J. A. Mauskopf, and M. C. Slack. 2009. "Rate, type, and cost of pelvic organ prolapse surgery in Germany, France, and England." *European Journal of Obstetrics & Gynecology and Reproductive Biology* 144 (2): 177-181.

van Raalte, H., and V. Egorov. 2015. "Tactile Imaging Markers to Characterize Female Pelvic Floor Conditions." *Open journal of obstetrics and gynecology* 5 (9): 505-515.

Weber, A. M., and H. E. Richter. 2005. "Pelvic Organ Prolapse." *Obstetrics & Gynecology* 106 (3): 615-634.

Wu, J. M., A. Kawasaki, A. F. Hundley, A. A. Dieter, E. R. Myers, and V. W. Sung. 2011. "Predicting the number of women who will undergo incontinence and prolapse surgery, 2010 to 2050." *Am J Obstet Gynecol* 205: 1-5.

Wu, J. M., C. A. Matthews, M. M. Conover, V. Pate, and M. J. Funk. 2014. “Lifetime Risk of Stress Incontinence or Pelvic Organ Prolapse Surgery.” *Obstetrics & Gynecology* 123 (6): 1201-1206.

APPENDIX A: Disassembled device